Functional and Molecular Characterisation of Mesenchymal Stem Cells Derived From Bone Marrow and Dental Tissues

Danijela Menicanin

Mesenchymal Stem Cell Research Group
Bone and Cancer Research Laboratory
Division of Haematology
Hanson Institute
Institute of Medical and Veterinary Sciences
SA Pathology

and

Colgate Australian Clinical Dental Research Centre
School of Dentistry
Faculty of Health Sciences
University of Adelaide

A thesis submitted to the University of Adelaide
for the degree of Doctor of Philosophy
June 2010

Chapter 4:

Gene Expression Profiling of Clonal BMSC, DPSC and PDLSC Populations

4. Gene Expression Profiling of Clonal Populations of BMSC, DPSC and PDLSC

Microarray technology presents a unique opportunity to gain insight into the biological complexity of cells and in turn has transformed the biological research landscape since its emergence 15 years ago [268, 269]. The introduction of high density gene array technology, in combination with the knowledge obtained from the sequencing of the human genome [180, 181], allows the assessment of global patterns of gene expression across multiple experimental samples and enables identification of major genomic differences and unique biological markers specific to the target cell populations [182].

The technology of microarrays can be integrated into many research areas and as such the employment of this application has undergone exponential growth since its introduction [270]. This technology has been widely applied in oncology research for assessing the molecular differences between malignant and normal cells, and in the identification of markers to aid the classification of tumours. Moreover, this technology has assisted in the identification of prognostic genes involved in tumour formation and progression. These are crucial elements to be addressed in cancer research and therapeutic developments targeted to cancer treatments [270]. Similarly, the use of microarrays has been applied to the study of infectious diseases to identify the mechanisms underlying molecular interactions that occur between the pathogen and the host. Identification of genes and hence regulatory pathways involved in pathogenesis of diseases can help in the development of targeted treatments [270]. Microarray technology has also been applied in the field of toxicology and pharmacology in determining the changes in gene expression patterns associated with exposures to quantified levels of toxicity. This approach can be used to identify the mechanisms of action of toxins and as such help in the development of risk assessment strategies associated with exposure to specific chemicals [270].

In cellular biology, the role of microarray technology in characterisation of cellular interactions at the molecular level, has had an important impact on deciphering biological processes involved in organ development and maintenance [270]. The advances in genomic profiling provide rapid and reliable data sets that define vital processes involved in cellular growth, survival and development that can be readily applied to different MSC-

like populations, following immunoselection and *ex vivo* expansion. Numerous research groups have utilised this technology to characterise MSCs at the genomic level and collectively these studies suggest that a cohort of genes are associated with stem cell functions and are thought to be involved in pathways that regulate stem cell maintenance as outlined in **Chapter 1, Section 1.4.**

The success of the development of microarray technology has resulted in design and production of multiple array types and accumulation of different platforms with varying features. As such, detailed planning of experiments should be considered prior to embarking on utilisation of microarray based approach for gene expression profiling. In light of previous research conducted on the assessment of various microarray platforms we decided to test the Affymetrix® U133 and Illumina® WG-6 platforms to assess gene expression patterns of our target cell populations.

Microarray technology is based on a detection system whereby specifically designed and labelled probes, deposited or synthesised onto glass, silicon or a nylon matrix, hybridise to the complementary DNA in the test samples. In this approach, the measured intensity of hybridisation represents the quantity of the target gene in the sample [271]. Affymetrix pioneered in the development of high density arrays, with the introduction of GeneChips, a unique technology of *in situ* oligonucleotide synthesis. In this process short single stranded DNA segments (25mer oligonucleotides) are synthesized onto the platform using combined techniques of photolithography and solid phase DNA synthesis [269]. The GeneChip® Human Genome U133 array used in this study represents over 14,500 human genes and analyzes the relative expression level of more than 18,400 transcripts. An alternate platform was developed by Illumina, which uses olginucleotides synthesised in the same way as initially used in spotted arrays, but employs a new array platform based on BeadArray technology [272]. This technology utilises the intrinsic size of a bead and patterned substrate, making the density of a bead 40 000 times higher than that of a typical spotted microarray. Furthermore, a novel, highly efficient strategy of bead labelling has been developed, eliminating the use of complex dye chemistries in the probe identification process [272]. The Human-6 Expression BeadChip® platform used in our experiments contains more than 46,000 probes derived from human genes. Other than the differences found in probe synthesis and physical attachment to the platform of the Affymetrix and Illumina technologies, further variations include probe selection and probe design [273]. In

platforms designed by Affymetrix, probes are synthesised at predefined locations on the platform and multiple probes are used for each gene whilst one-base mismatch probes are used as internal controls of non specific hybridisation. On the other hand, Illumina uses 30 copies of the same oligonucleotide on the array which provides a high level of internal technical replication and randomly generated arrays undergo a 'decoding step' to identify each probe based on its assigned molecular address. Individual Affymetrix arrays are positioned on separate substrates and are in turn processed separately, whilst multiple Illumina arrays (6 or 8) are placed on the same physical substrate, allowing for the processing of samples to be performed simultaneously [273].

The initial aim of this study was to compare microarray analyses between Affymetrix® U133 and Illumina® WG-6 platforms. This was investigated by assessing and comparing gene expression profiles of long-lived/multi-potential and lowly proliferative clonal populations of PDLSCs across the two platforms. MSC clones derived from periodontal ligament were used in this experiment as this was the first populations from which a set of three clones of low growth and three clones of high growth and multi-differentiation potential were obtained. Following this initial assessment, we aimed to identify differentially expressed genes unique to immature, high proliferating, multi-potential MSC-like clonal populations for BMSCs, DPSCs and PDLSCs. To achieve this, we compared the growth and differentiation of stem/progenitor cells and their progeny contained within clonal BMSC, DPSC and PDLSC populations using a global microarray analysis strategy.

4.1. Results

4.1.1. Comparison of Microarray Platforms Designed by Illumina and Affymetrix in Genomic Profiling of PDLSC Clonal Lines

Comparative genomic analysis was performed using commercial Affymetrix® U133 and Illumina® WG-6 platforms, on three biological replicates of PDLSC clonal cell lines exhibiting low growth potential and compared with three PDLSC clones of high growth/multi-differentiation potentials. The analyses obtained from Affymetrix® U133 and Illumina® WG-6 platforms identified 1,000 and 842 differentially expressed genes between the different clonal populations, respectively (**Figure 4.1**) Statistical analysis of the Affymetrix generated data was performed using Partek Genomics Suite software

Figure 4.1 Comparison of Gene Expression Profiling of PDLSCs using Affymetrix U133 and Illumina WG-6 Microarray Platforms.

Gene expression profiles of PDLSC of high growth/multi-differentiation potential and PDLSC of low growth potential were generated using Affymetrix U133 and Illumina WG-6 microarray platforms. The data were interrogated to identify statistically significant differentially expressed genes obtained from each of the two different microarray analysis platforms and further cross-analysed to identify genes common to both systems.

Figure 4.1

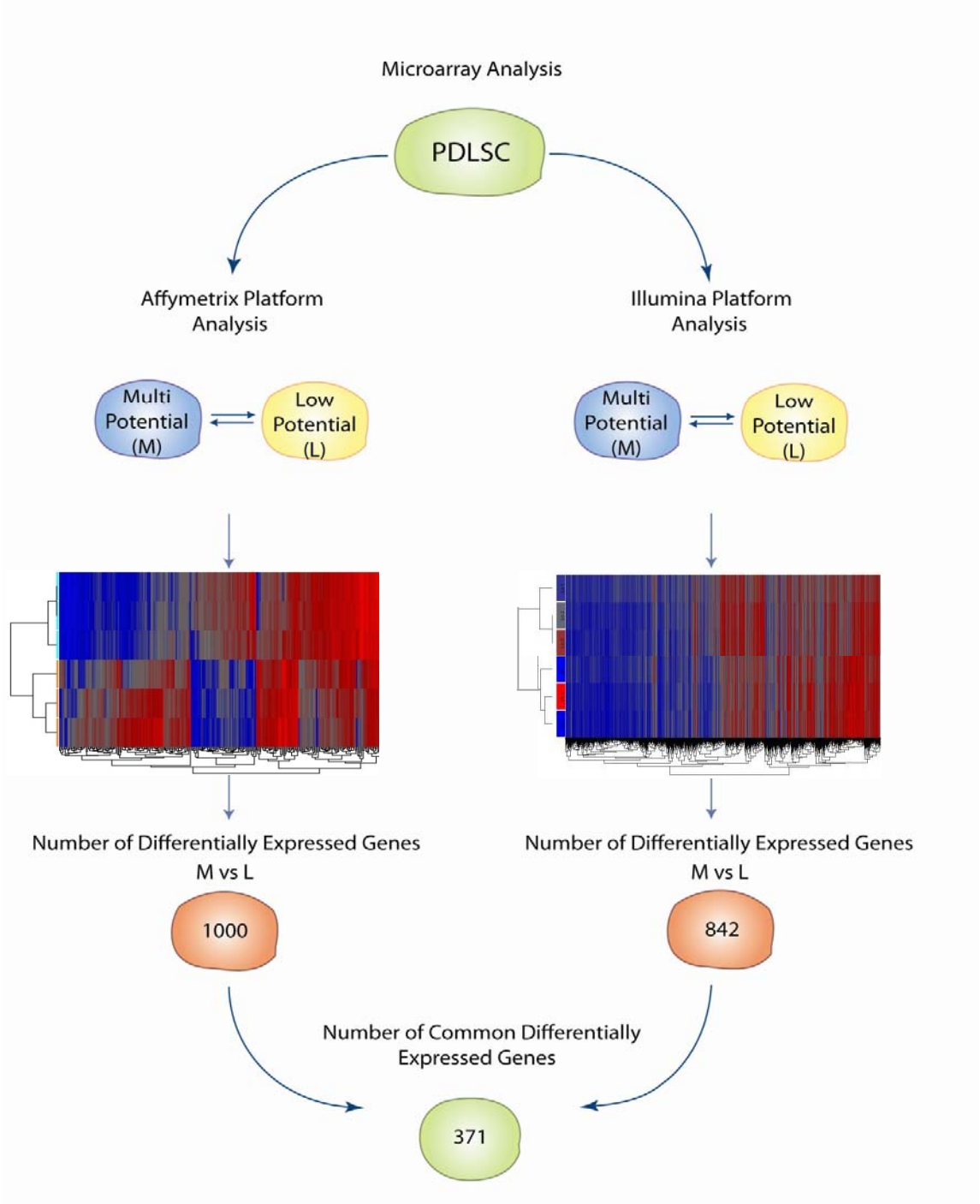
Microarray Analysis
PDLSC
Affymetrix Platform Analysis
Illumina Platform Analysis
Multi Potential (M)
Low Potential (L)
Multi Potential (M)
Low Potential (L)
Number of Differentially Expressed Genes M vs L
1000
Number of Differentially Expressed Genes M vs L
842
Number of Common Differentially Expressed Genes
371

(Partek Inc. St. Louis, MI, USA). Statistical analysis of data generated using Illumina was performed using lumi package in R statistical software [232, 233] and GeneSpring GX (Agilent Technologies, Forest Hill, VIC, Australia). In further cross comparison of this data, we identified 371 genes common to analyses performed on both of the platforms. These comparisons were performed using Microsoft® Office Excel® 2007 (software version 12.0.6524.5003, Microsoft Corporation).

Given the similarities in the sensitivity of the two microarray platforms, subsequent studies used the Illumina® WG-6 platform which allowed for the parallel interrogation of six RNA samples. This approach was particularly suitable to our experimental design where we compared three biological replicates of low growth potential clonal cell lines with three clones exhibiting high growth/multi-differentiation potentials, for each tissue type.

4.1.2. Genomic Profiling of BMSC, DPSC and PDLSC Clonal Lines Exhibiting Differential Growth and Developmental Potentials

To identify genes involved in MSC maintenance, growth and development we used large-scale gene expression profiling using a commercial Illumina® WG-6 platform, on three biological replicates of clonal cell lines exhibiting low growth potential compared with three clones exhibiting high growth/multi-differentiation potentials, for each of the three tissue types. The differentiation capacity of long lived BMSC, DPSC and PDLSC clones following culture in osteogenic, adipogenic and chondrogenic induction media, was confirmed by quantitative analysis of extracellular matrix calcium concentration, triglyceride levels and measurement of GAG synthesis, respectively (**Figure 4.2**). Comparative genomic analysis was performed based on three biological replicate clones for each tissue (**Figures 4.3-4.5).**

Lumi package in R statistical software and GeneSpring GX software were used for statistical analysis, where a cut off point with a p-value of 0.05 was used to identify statistically significant differentially expressed genes. These bioinformatic analyses identified 968, 603 and 842 differentially expressed genes between low growing clones and high growth/multi-differentiation potential clones for BMSC, DPSC and PDLSC, respectively **(Figure 4.6)**.

Figure 4.2 Comparison of the Developmental Potential of Different Long Lived MSC-like clones.

Three clonal cell populations of long lived BMSC, DPSC and PDLSC were assessed for their capacity to undergo osteogenic, adipogenic and chondrogenic differentiation. (**A**) Calcium levels within the extracellular matrix were measured and normalized to DNA content per well following osteogenic induction. (**B**) Oil red O positive triglycerides were measured and normalized to DNA content per well following adipogenic induction. (**C**) Glycosaminoglycan synthesis was measured and normalized to DNA content per well following induction with chondrogenic inductive media. The data represents the mean values ± standard errors of triplicate experiments generated from three different BMSC, DPSC and PDLSC clonal populations.

Figure 4.2

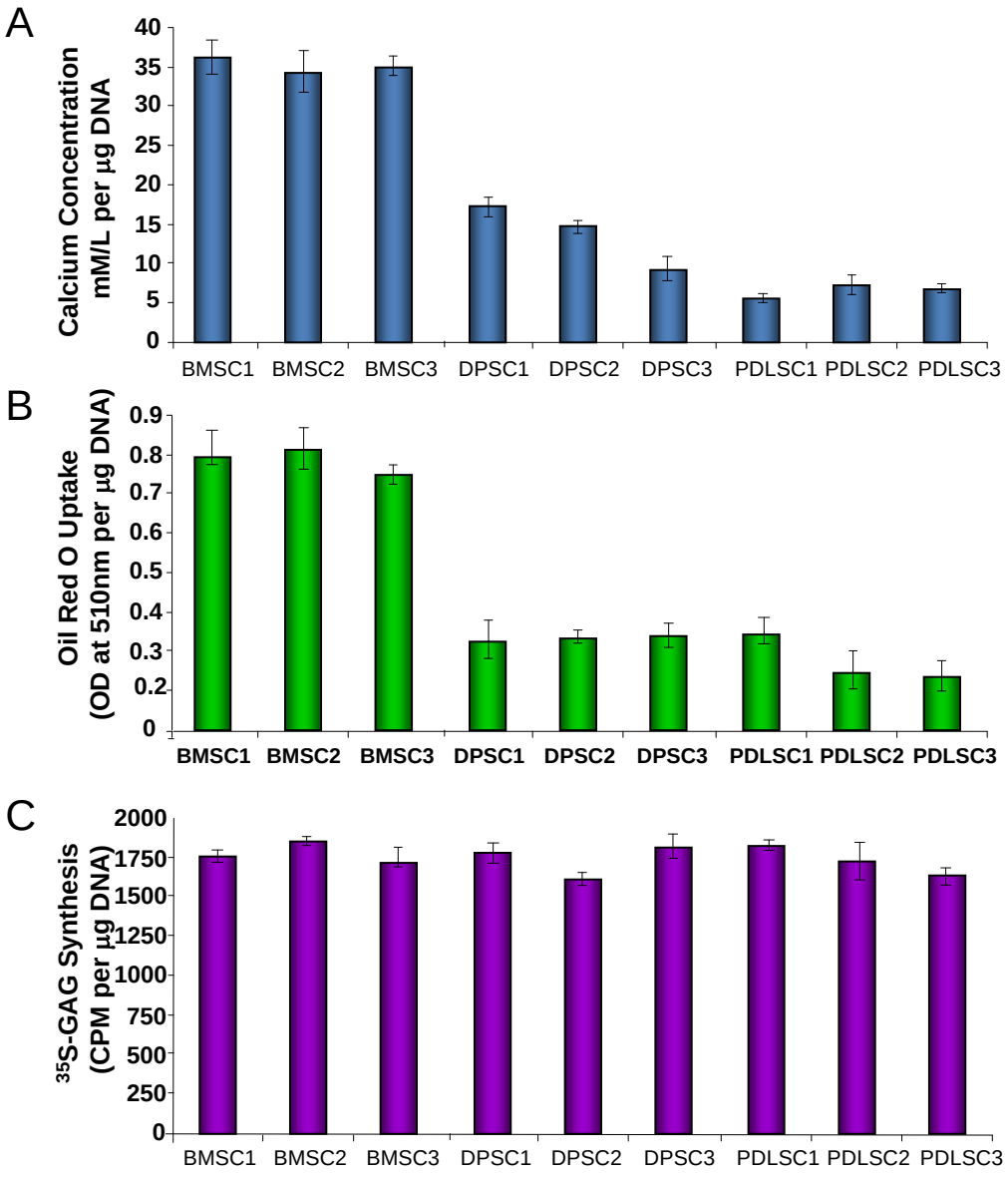
A
Calcium Concentration mM/L per µg DNA
40
35
30
25
20
15
10
5
0
BMSC1 BMSC2 BMSC3 DPSC1 DPSC2 DPSC3 PDLSC1 PDLSC2 PDLSC3
B
Oil Red O Uptake (OD at 510nm per µg DNA)
0.9
0.8
0.7
0.6
0.5
0.4
0.3
0.2
0
BMSC1 BMSC2 BMSC3 DPSC1 DPSC2 DPSC3 PDLSC1 PDLSC2 PDLSC3
C
35S-GAG Synthesis (CPM per µg DNA)
2000
1750
1500
1250
1000
750
500
250
0
BMSC1 BMSC2 BMSC3 DPSC1 DPSC2 DPSC3 PDLSC1 PDLSC2 PDLSC3

Figure 4.3 Hierarchical Sample Clustering of BMSC Clones.

(**A**) The representative dendrogram illustrates patterns of gene expression levels, of significant differentially expressed genes within the samples analysed for the BMSC population. Clones 1 to 3 represent clones of low growth potential (<20 population doublings), whilst clones 4 to 6 represent clones of high growth potential (>20 population doublings). (**B**) Representative scatterplot diagrams illustrate patterns of gene expression levels of (**i**) all of the genes represented on the microarray platform and (**ii**) statistically significant differentially expressed genes within the samples analysed for the BMSC population. Lumi package in R statistical software and GeneSpring GX were used for statistical analysis and a p-value of 0.05 was used as a cut off point to identify statistically significant differentially expressed genes with greater than 2 fold difference.

Figure 4.3

A

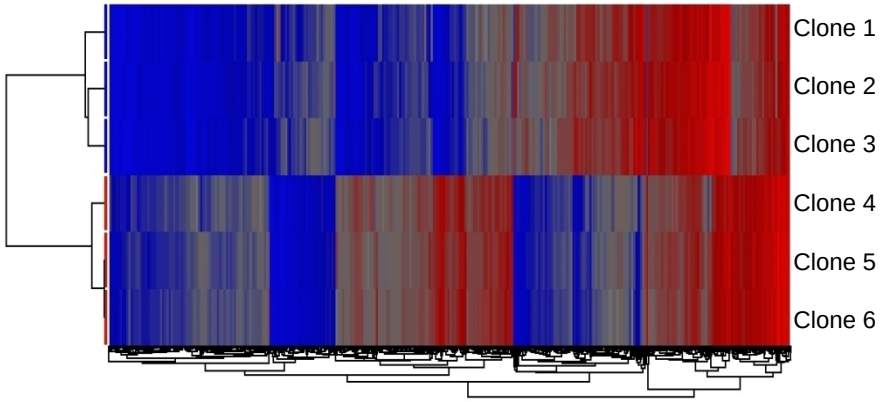
Clone 1
Clone 2
Clone 3
Clone 4
Clone 5
Clone 6

B

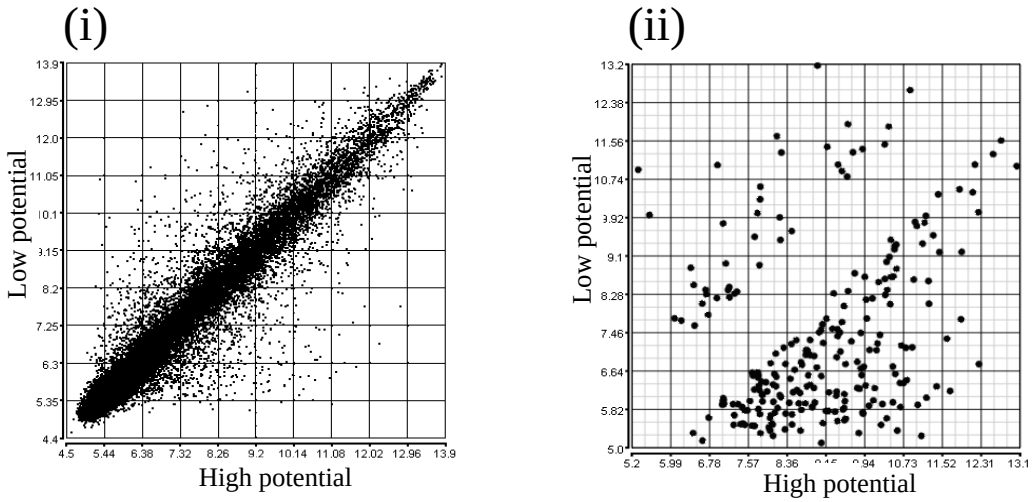
(i)
(ii)
Low potential
High potential
Low potential
High potential

Figure 4.4 Hierarchical Sample Clustering of DPSC Clones.

(**A**) The representative dendrogram illustrates patterns of gene expression levels, of significant differentially expressed genes within the samples analysed for the DPSC population. Clones 1 to 3 represent clones of low growth potential (<20 population doublings), whilst clones 4 to 6 represent clones of high growth potential (>20 population doublings). (**B**) Representative scatterplot diagrams illustrate patterns of gene expression levels of (**i**) all of the genes represented on the microarray platform and (**ii**) statistically significant differentially expressed genes within the samples analysed for the DPSC population.Lumi package in R statistical software and GeneSpring GX were used for statistical analysis and a p-value of 0.05 was used as a cut off point to identify statistically significant differentially expressed genes with greater than 2 fold difference.

Figure 4.4

A

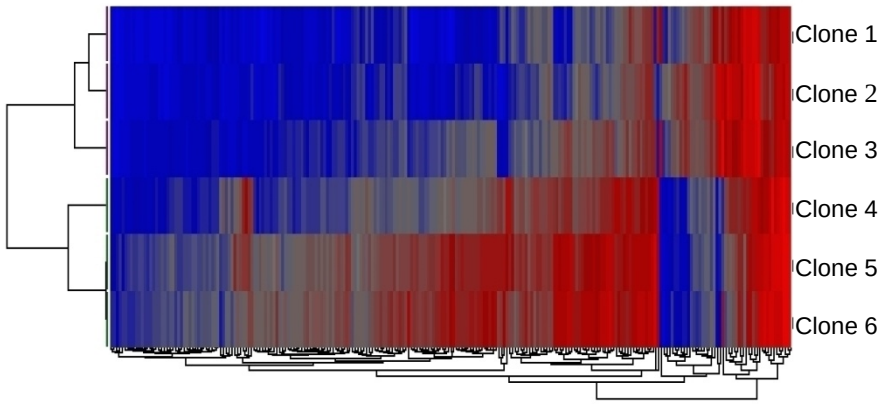
Clone 1
Clone 2
Clone 3
Clone 4
Clone 5
Clone 6

B

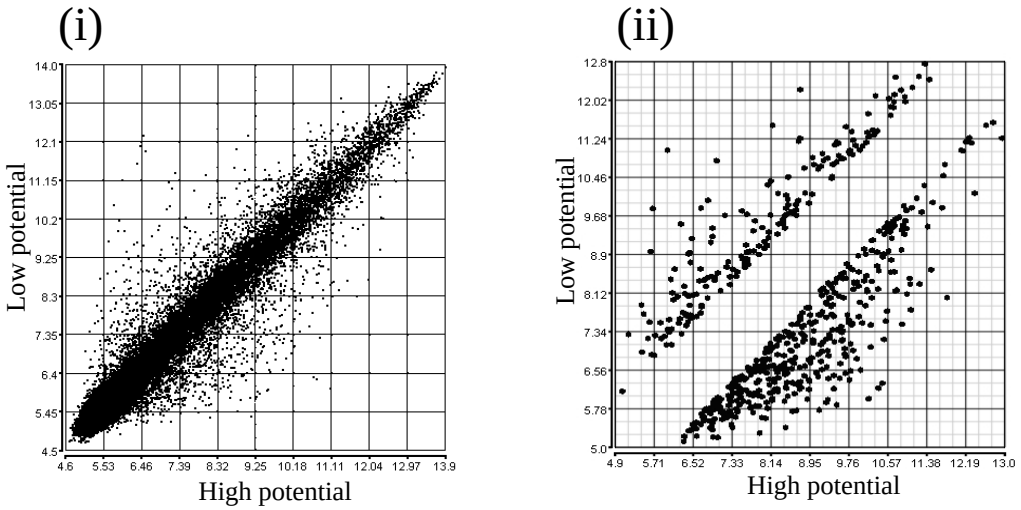
(i)
(ii)
Low potential
High potential
14.0
13.05
12.1
11.15
10.2
9.25
8.3
7.35
6.4
5.45
4.5
4.6 5.53 6.46 7.39 8.32 9.25 10.18 11.11 12.04 12.97 13.9
12.8
12.02
11.24
10.46
9.68
8.9
8.12
7.34
6.56
5.78
5.0
4.9 5.71 6.52 7.33 8.14 8.95 9.76 10.57 11.38 12.19 13.0

Figure 4.5 Hierarchical Sample Clustering of PDLSC Clones.

(**A**) The representative dendrogram illustrates patterns of gene expression levels, of significant differentially expressed genes within the samples analysed for the PDLSC population. Clones 1 to 3 represent clones of low growth potential (<20 population doublings), whilst clones 4 to 6 represent clones of high growth potential (>20 population doublings). (**B**) Representative scatterplot diagrams illustrate patterns of gene expression levels of (**i**) all of the genes represented on the microarray platform and (**ii**) statistically significant differentially expressed genes within the samples analysed for the DPSC population. Lumi package in R statistical software and GeneSpring GX were used for statistical analysis and a p-value of 0.05 was used as a cut off point to identify statistically significant differentially expressed genes with greater than 2 fold difference.

Figure 4.5

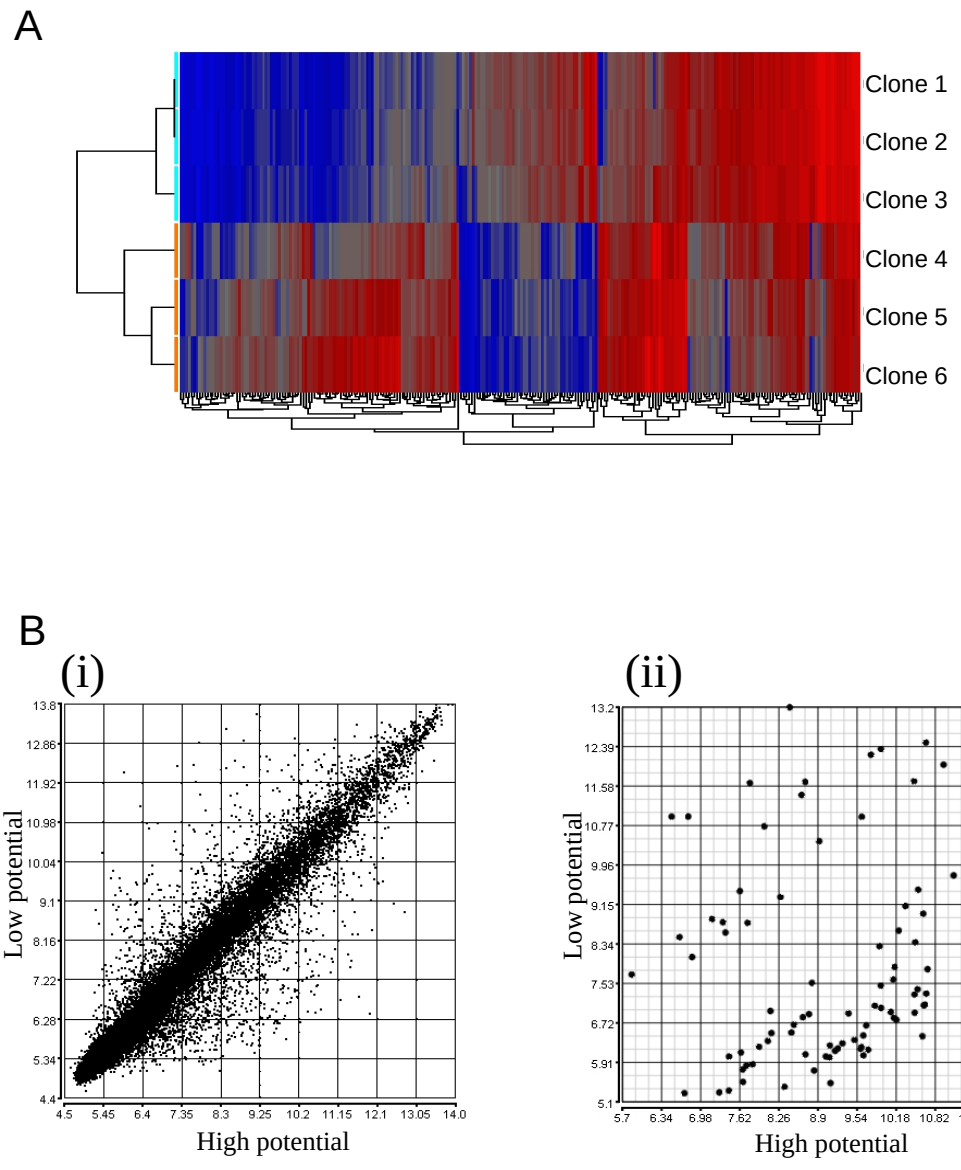
A
Clone 1
Clone 2
Clone 3
Clone 4
Clone 5
Clone 6
B
(i)
Low potential
High potential
13.8
12.86
11.92
10.98
10.04
9.1
8.16
7.22
6.28
5.34
4.4
4.5
5.45
6.4
7.35
8.3
9.25
10.2
11.15
12.1
13.05
14.0
(ii)
Low potential
High potential
13.2
12.39
11.58
10.77
9.96
9.15
8.34
7.53
6.72
5.91
5.1
5.7
6.34
6.98
7.62
8.26
8.9
9.54
10.18
10.82
11.46
12.1

Figure 4.6 Schematic Presentation of the Microarray Analysis Approach Used in the Study

Gene expression profiles of MSCs of high growth/multi-differentiation potential and MSCs of low growth potential were generated and compared across BMSC, DPSC and PDLSC populations, using microarray analysis. The data was interrogated to identify statistically significant differentially expressed genes common to all three cell populations as represented in the Venn diagram.

Figure 4.6

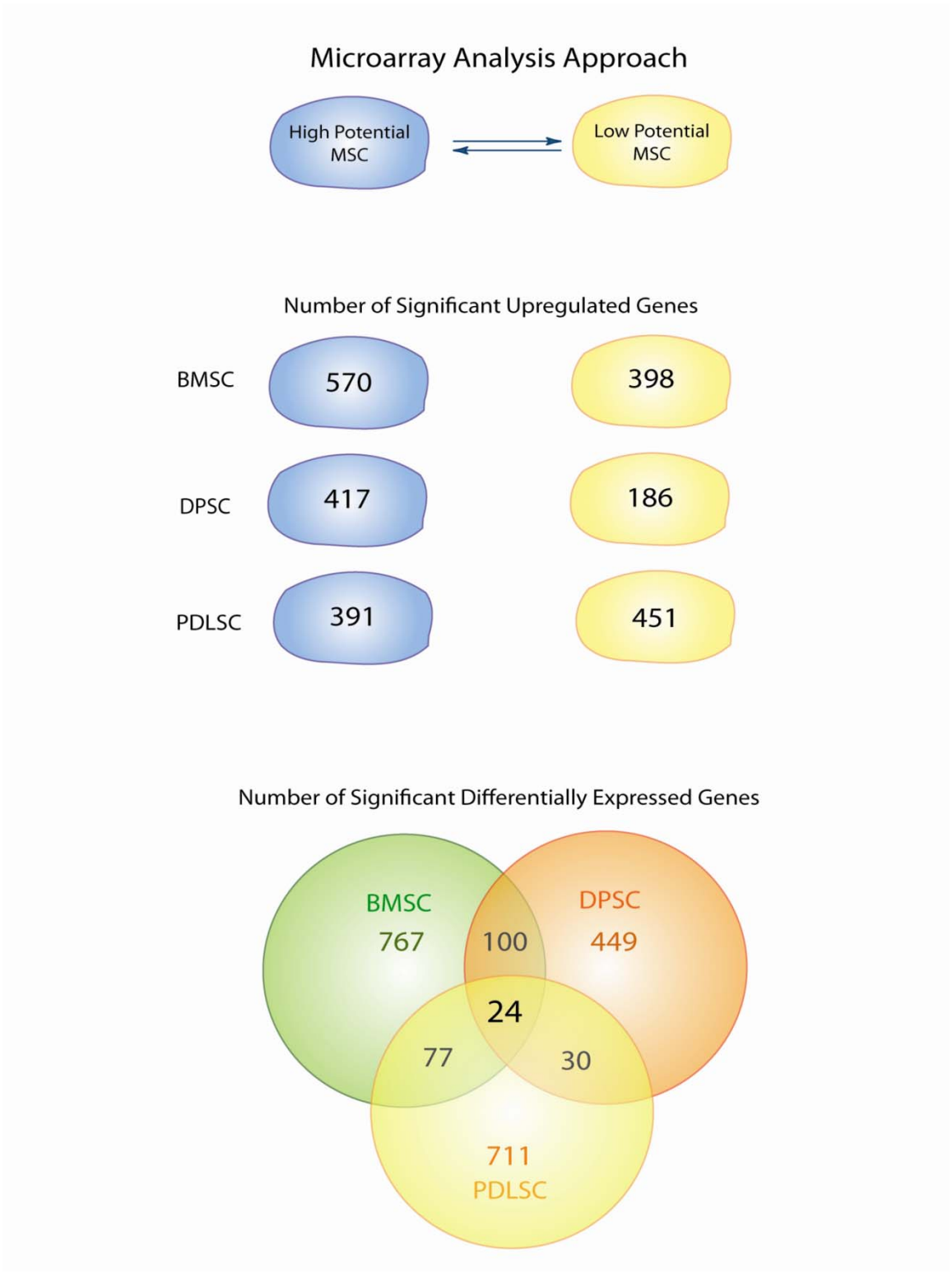
Microarray Analysis Approach
High Potential MSC
Low Potential MSC
Number of Significant Upregulated Genes
BMSC
570
398
DPSC
417
186
PDLSC
391
451
Number of Significant Differentially Expressed Genes
BMSC
767
100
DPSC
449
24
77
30
711
PDLSC

4.1.3. Identification of Common Gene Sets Expressed by Long Lived, Multi-Potent BMSC, DPSC and PDLSC Clonal Lines

Further cross-comparison analyses were performed to identify differentially expressed genes that were commonly expressed amongst long lived, multi-potent cell populations derived from the three different stromal tissues. A simultaneous search across three spreadsheets of data generated by the AGRF (Melbourne, VIC, Australia) was performed to match the corresponding genes across the three populations, hence identify differentially expressed genes common to MSC derived from the bone marrow, dental pulp and periodontal ligament tissues. These analyses were performed using Microsoft® Office Excel® 2007 (software version 12.0.6524.5003, Microsoft Corporation). Interrogation of the data resulted in the identification of 24 common differentially upregulated genes that could be grouped into categories based on their involvement in different cellular processes, including cell cycle, mitosis and cell division, DNA repair and replication and cellular differentiation (**Table 4.1)**. The values in the table represent increases in fold changes of gene expression in MSCs of high growth and multi-differentiation potential. Within this gene data set, the transcription factors, E2F-2, PTTG-1, TWIST-1 and transcriptional co-factor, LDB-2 were found to be commonly upregulated in long lived, multi-potent cells derived from all three tissues. Confirmatory studies using real-time PCR analysis were performed to validate the microarray findings for those genes involved in transcriptional regulation. (**Figure 4.7)**. Real-Time PCR analysis was also performed to verify the differential gene expression patterns observed for the other 20 highly expressed stem cell associated genes **(Figures 4.8 - 4.12)**.

We compared gene expression patterns of four transcription related factors between multi-potential BMSCs, DPSCs, PDLSCs and high proliferative human foreskin fibroblasts (HFF) which lack the capacity to differentiate into, bone, fat and cartilage. These data showed that the expression of LDB2, PTTG1 and TWIST1 was significantly higher in multi-potential BMSCs, DPSCs and PDLSCs in comparison to HFF. However, the expression of E2F2 was highest for HFF, where E2F family members play a major role in regulation of cellular proliferation (**Figure 4.13**). Elevated levels of E2F2 were also correlated with the faster growing rate of HFF compared to to the different MSC-like populations (data not shown).

Table 4.1 A List of Genes Up-Regulated in Cell Clones of High Potential, Common to BMSC, DPSC and PDLSC Populations.

Gene	*Gene Name*	BMSCs	DPSCs	PDLSCs
Genes involved in cell cycle, mitosis, cell division				
ASPM	*asp (abnormal spindle) homolog*	18.08	6.049	5.834
AURKB	*aurora kinase B*	9.895	5.145	6.953
CCNB2	*cyclin B2*	34.09	7.838	6.39
CDC2	*cell division cycle 2, G1 to S and G2 to M*	11.61	5.883	2.537
CDC20	*cell division cycle 20 homolog (S. cerevisiae)*	44.6	13.65	7.844
CENPF	*centromere protein F, 350/400ka (mitosin)*	17.5	6.135	6.539
CEP55	*centrosomal protein 55kDa*	17.48	7.228	5.436
CIT	*citron (rho-interacting, serine/threonine kinase 21)*	6.154	2.512	2.728
CKS2	*CDC28 protein kinase regulatory subunit 2*	12.78	4.736	4.311
DLG7	*discs, large (Drosophila) homolog-associated protein 5*	22.57	7.546	6.32
MAD2L1	*MAD2 mitotic arrest deficient-like 1 (yeast)*	7.696	4.89	5.263
NCAPG	*non-SMC condensin I complex, subunit G*	15.86	6.747	7.558
PBK	*PDZ binding kinase*	37.95	10.62	12.09
PTTG1	*pituitary tumor-transforming 1*	18.06	6.098	5.537
UBE2C	*ubiquitin-conjugating enzyme E2C*	27.73	7.399	7.936
Genes involved in DNA repair and replication				
CHEK1	*CHK1 checkpoint homolog (S. pombe)*	4.744	3.09	3.187
E2F2	*E2F transcription factor 2*	5.999	5.594	6.07
GINS2	*GINS complex subunit 2 (Psf2 homolog)*	14.44	5.737	6.466
POLQ	*polymerase (DNA directed), theta*	7.984	3.397	5.398
PTTG1	*pituitary tumor-transforming 1*	18.06	6.098	5.537
RPA3	*replication protein A3, 14kDa*	2.335	2.173	2.036
RRM2	*ribonucleotide reductase M2 polypeptide*	7.035	5.318	7.749
TOP2A	*topoisomerase (DNA) II alpha 170kDa*	44.64	10.38	10.32
Genes involved in regulation of transcription				
CENPF	*centromere protein F, 350/400ka (mitosin)*	17.5	6.135	6.539
E2F2	*E2F transcription factor 2*	5.999	5.594	6.07
LDB2	*LIM domain binding 2*	3.313	3.066	4.981
PTTG1	*pituitary tumor-transforming 1*	18.06	6.098	5.537
TWIST1	*twist homolog 1 (Drosophila)*	2.064	3.151	2.297
Genes involved in cell proliferation and differentiation				
CENPF	*centromere protein F, 350/400ka (mitosin)*	17.5	6.135	6.539
CHEK1	*CHK1 checkpoint homolog (S. pombe)*	4.744	3.09	3.187
CIT	*citron (rho-interacting, serine/threonine kinase 21)*	6.154	2.512	2.728
CKS2	*CDC28 protein kinase regulatory subunit 2*	12.78	4.736	4.311
TWIST1	*twist homolog 1 (Drosophila)*	2.064	3.151	2.297

Figure 4.7 Confirmation of Microarray Data for Genes Associated with Transcription by Real-Time PCR.

Representative graphs of Real-Time PCR analysis of expression levels of regulators of transcription, E2F-2, LDB-2, PTTG-1 and TWIST-1, confirm up-regulation of these genes in high growth/multi-differentiation potential clones in comparison to low growth potential clones, as primarily identified in microarray analysis. The data represent the mean values ± standard deviations of triplicate experiments normalized to the house keeping β-actin gene. Statistical significance of (Δ) $p<0.001$ and (*) $p<0.0001$ was determined using the unpaired student t-test.

Figure 4.7

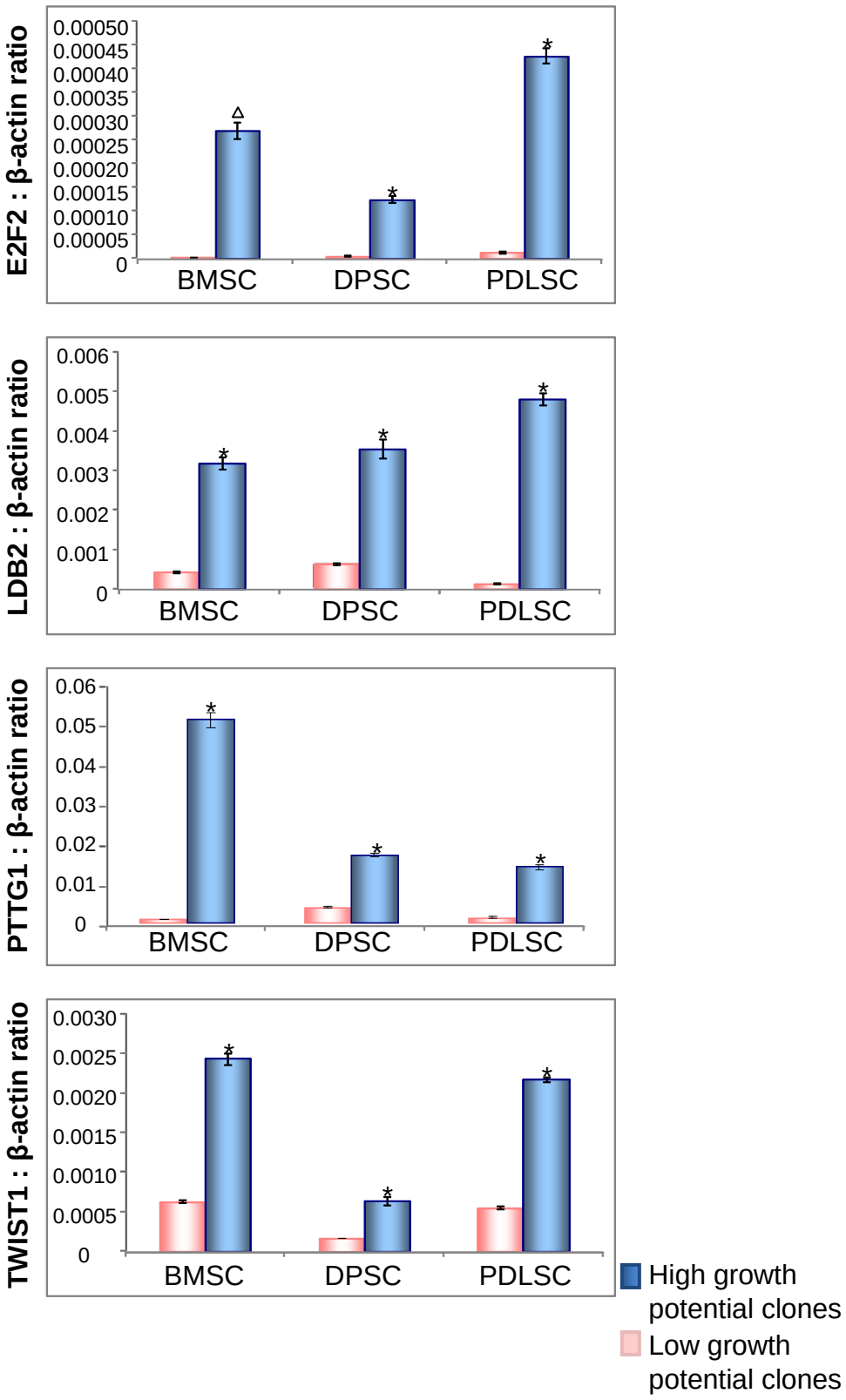
E2F2 : β-actin ratio
0.00050
0.00045
0.00040
0.00035
0.00030
0.00025
0.00020
0.00015
0.00010
0.00005
0
BMSC
DPSC
PDLSC
LDB2 : β-actin ratio
0.006
0.005
0.004
0.003
0.002
0.001
0
BMSC
DPSC
PDLSC
PTTG1 : β-actin ratio
0.06
0.05
0.04
0.03
0.02
0.01
0
BMSC
DPSC
PDLSC
TWIST1 : β-actin ratio
0.0030
0.0025
0.0020
0.0015
0.0010
0.0005
0
BMSC
DPSC
PDLSC
High growth potential clones
Low growth potential clones

Figure 4.8 Confirmation of ASPM, AURKB, CCNB2 and CDC2 Expression by Real-Time PCR.

Representative graphs of Real-Time PCR analysis of expression levels of differentially expressed genes, ASPM, AURKB, CCNB2 and CDC2, confirm up-regulation of these genes in high growth/multi-differentiation potential clones in comparison to low growth potential clones. The data represent the mean values ± standard deviations of triplicate experiments normalized to the house keeping β-actin gene. Statistical significance of (Δ) $p<0.001$ and (*) $p<0.0001$ was determined using the unpaired student t-test.

Figure 4.8

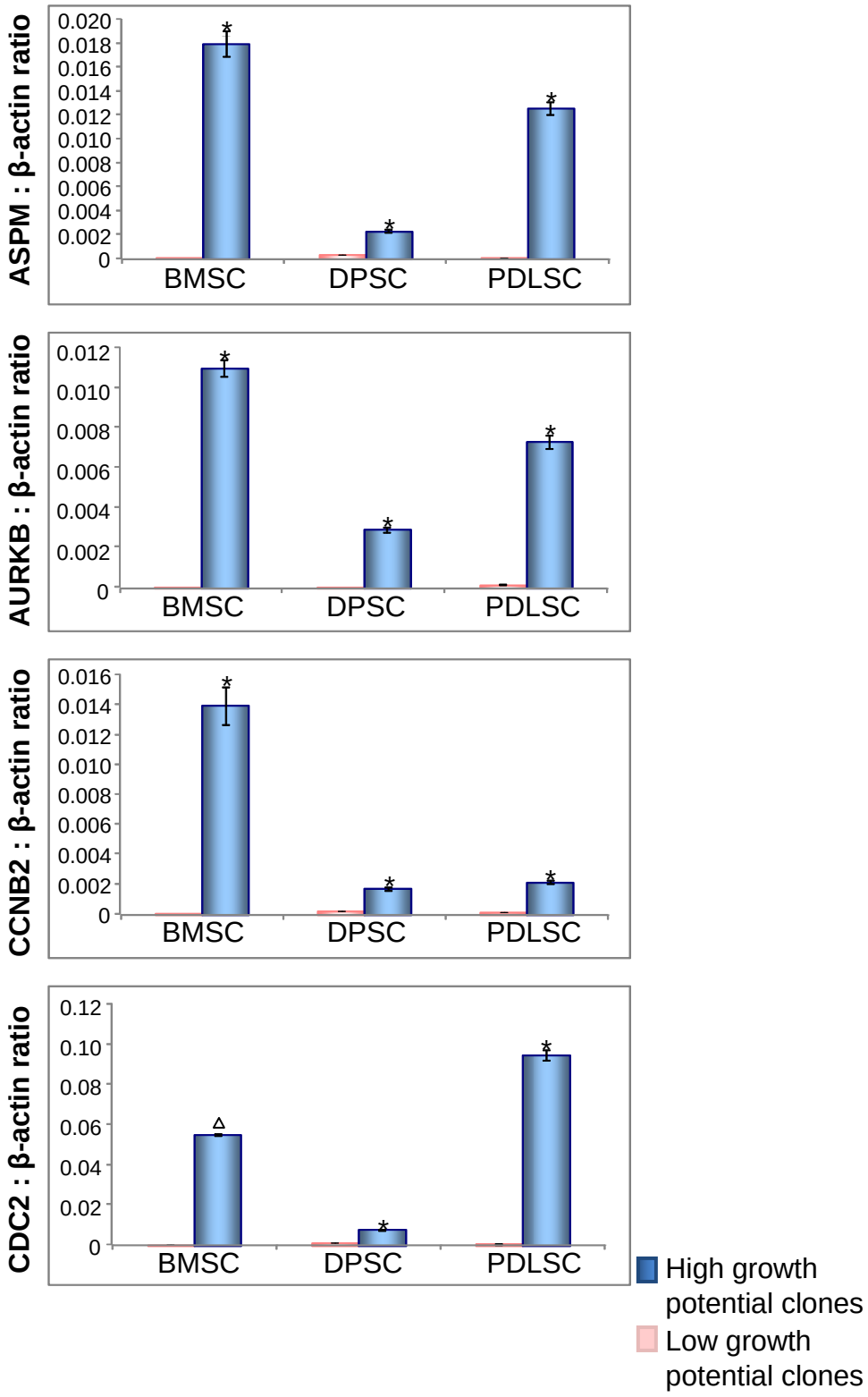
ASPM : β-actin ratio
0.020
0.018
0.016
0.014
0.012
0.010
0.008
0.006
0.004
0.002
0
BMSC
DPSC
PDLSC
AURKB : β-actin ratio
0.012
0.010
0.008
0.006
0.004
0.002
0
BMSC
DPSC
PDLSC
CCNB2 : β-actin ratio
0.016
0.014
0.012
0.010
0.008
0.006
0.004
0.002
0
BMSC
DPSC
PDLSC
CDC2 : β-actin ratio
0.12
0.10
0.08
0.06
0.04
0.02
0
BMSC
DPSC
PDLSC
High growth potential clones
Low growth potential clones

Figure 4.9 Confirmation of CDC20, CENPF, CEP55 and CHEK1 Expression by Real-Time PCR.

Representative graphs of Real-Time PCR analysis of expression levels of differentially expressed genes, CDC20, CENPF, CEP55 and CHEK1, confirm up-regulation of these genes in high growth/multi-differentiation potential clones in comparison to low growth potential clones. The data represent the mean values ± standard deviations of triplicate experiments normalized to the house keeping β-actin gene. Statistical significance of (*) $p<0.0001$ was determined using the unpaired student t-test.

Figure 4.9

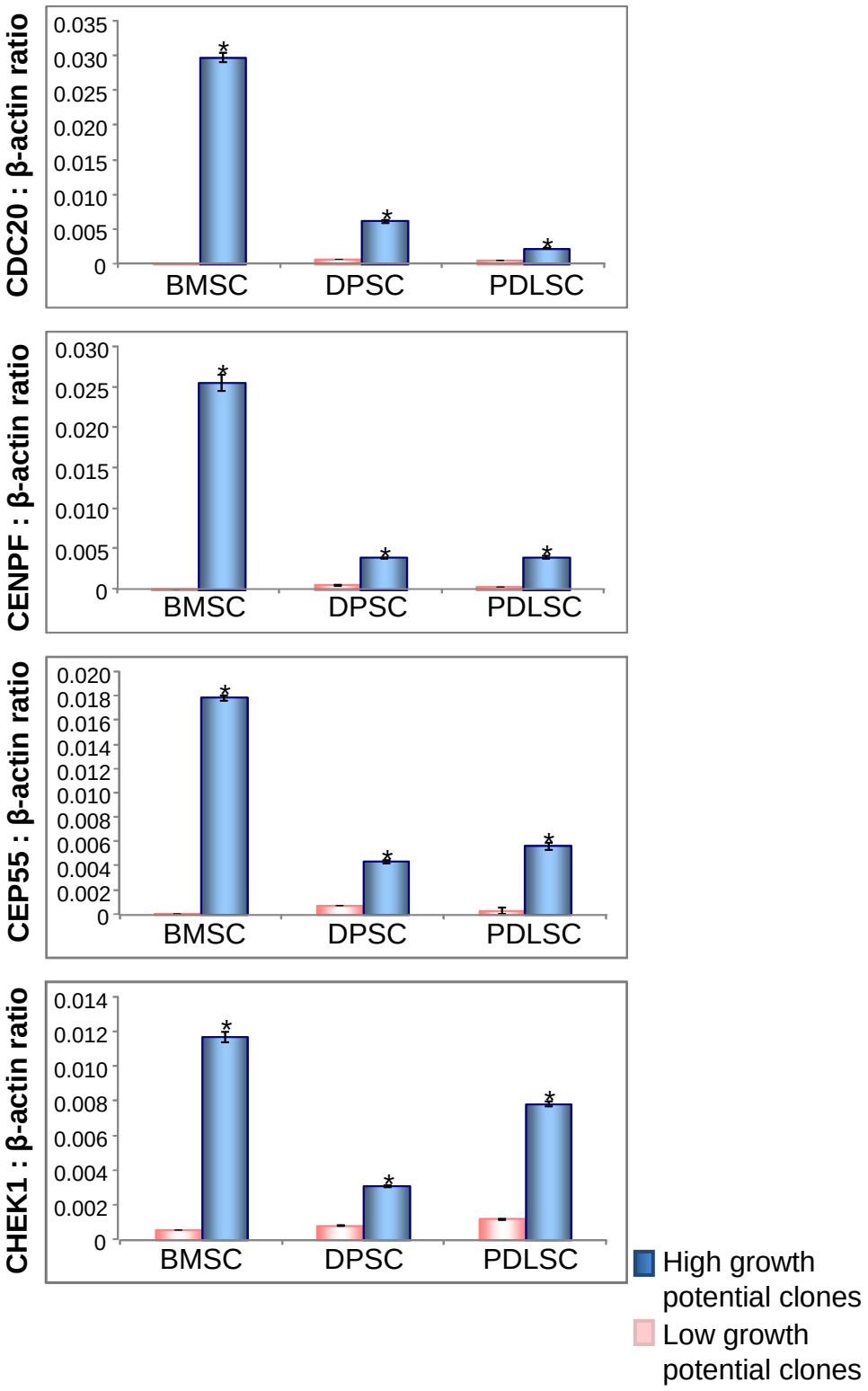
CDC20 : β-actin ratio
0.035
0.030
0.025
0.020
0.015
0.010
0.005
0
BMSC
DPSC
PDLSC
CENPF : β-actin ratio
0.030
0.025
0.020
0.015
0.010
0.005
0
BMSC
DPSC
PDLSC
CEP55 : β-actin ratio
0.020
0.018
0.016
0.014
0.012
0.010
0.008
0.006
0.004
0.002
0
BMSC
DPSC
PDLSC
CHEK1 : β-actin ratio
0.014
0.012
0.010
0.008
0.006
0.004
0.002
0
BMSC
DPSC
PDLSC
High growth potential clones
Low growth potential clones

Figure 4.10 Confirmation of CIT, CKS2, DLG7 and GINS2 Expression by Real-Time PCR.

Representative graphs of Real-Time PCR analysis of expression levels of differentially expressed genes, CIT, CKS2, DLG7 and GINS2, confirm up-regulation of these genes in high growth/multi-differentiation potential clones in comparison to low growth potential clones. The data represent the mean values ± standard deviations of triplicate experiments normalized to the house keeping β-actin gene. Statistical significance of (Δ) $p<0.001$ and (*) $p<0.0001$ was determined using the unpaired student t-test.

Figure 4.10

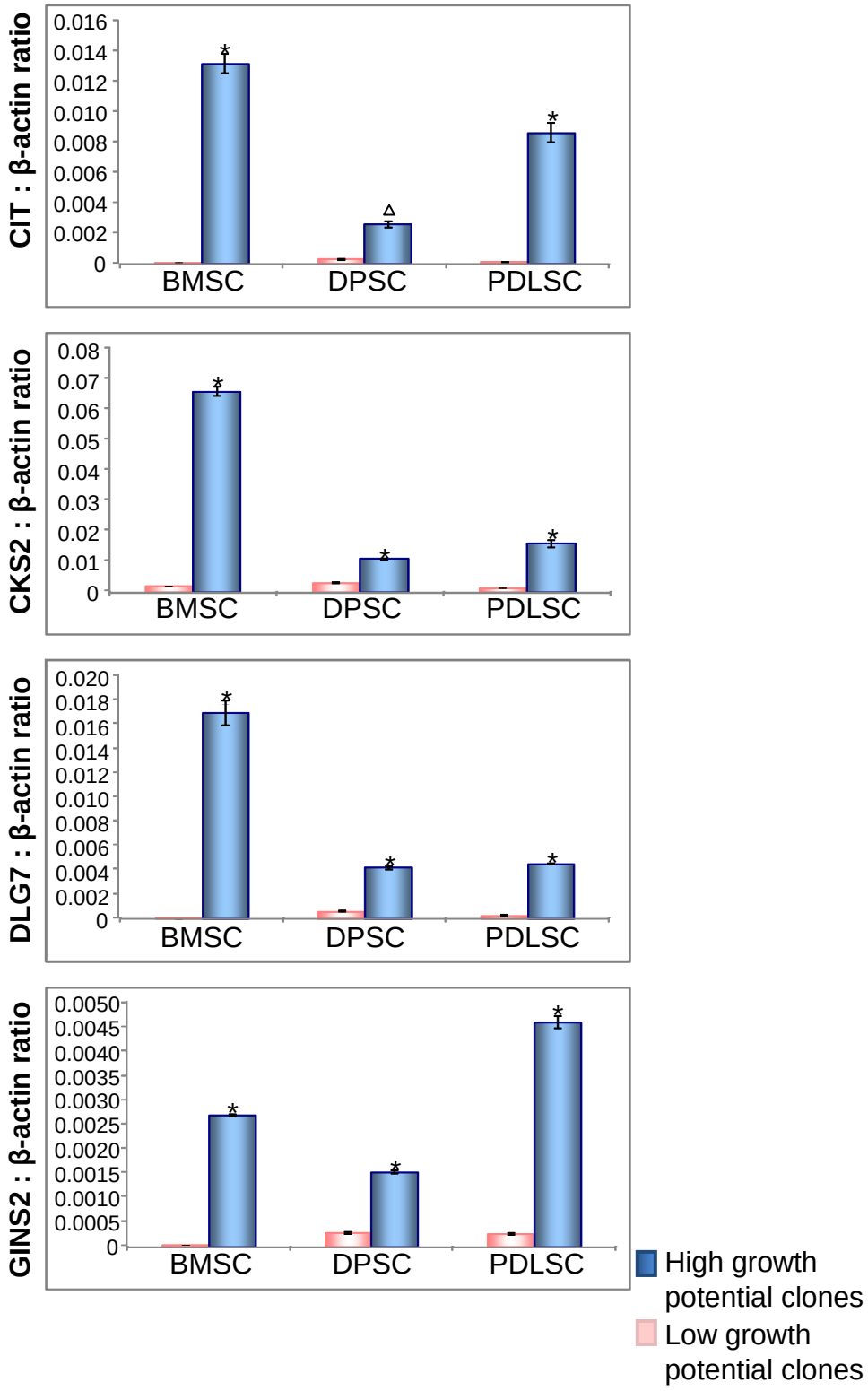
CIT : β-actin ratio
0.016
0.014
0.012
0.010
0.008
0.006
0.004
0.002
0
BMSC
DPSC
PDLSC
CKS2 : β-actin ratio
0.08
0.07
0.06
0.05
0.04
0.03
0.02
0.01
0
BMSC
DPSC
PDLSC
DLG7 : β-actin ratio
0.020
0.018
0.016
0.014
0.012
0.010
0.008
0.006
0.004
0.002
0
BMSC
DPSC
PDLSC
GINS2 : β-actin ratio
0.0050
0.0045
0.0040
0.0035
0.0030
0.0025
0.0020
0.0015
0.0010
0.0005
0
BMSC
DPSC
PDLSC
High growth potential clones
Low growth potential clones

Figure 4.11 Confirmation of MAD2L, NCAPG, PBK and POLQ Expression by Real-Time PCR.

Representative graphs of Real-Time PCR analysis of expression levels of differentially expressed genes, MAD2L, NCAPG, PBK and POLQ, confirm up-regulation of these genes in high growth/multi-differentiation potential clones in comparison to low growth potential clones. The data represent the mean values ± standard deviations of triplicate experiments normalized to the house keeping β-actin gene. Statistical significance of (Δ) $p<0.001$ and (*) $p<0.0001$ was determined using the unpaired student t-test.

Figure 4.11

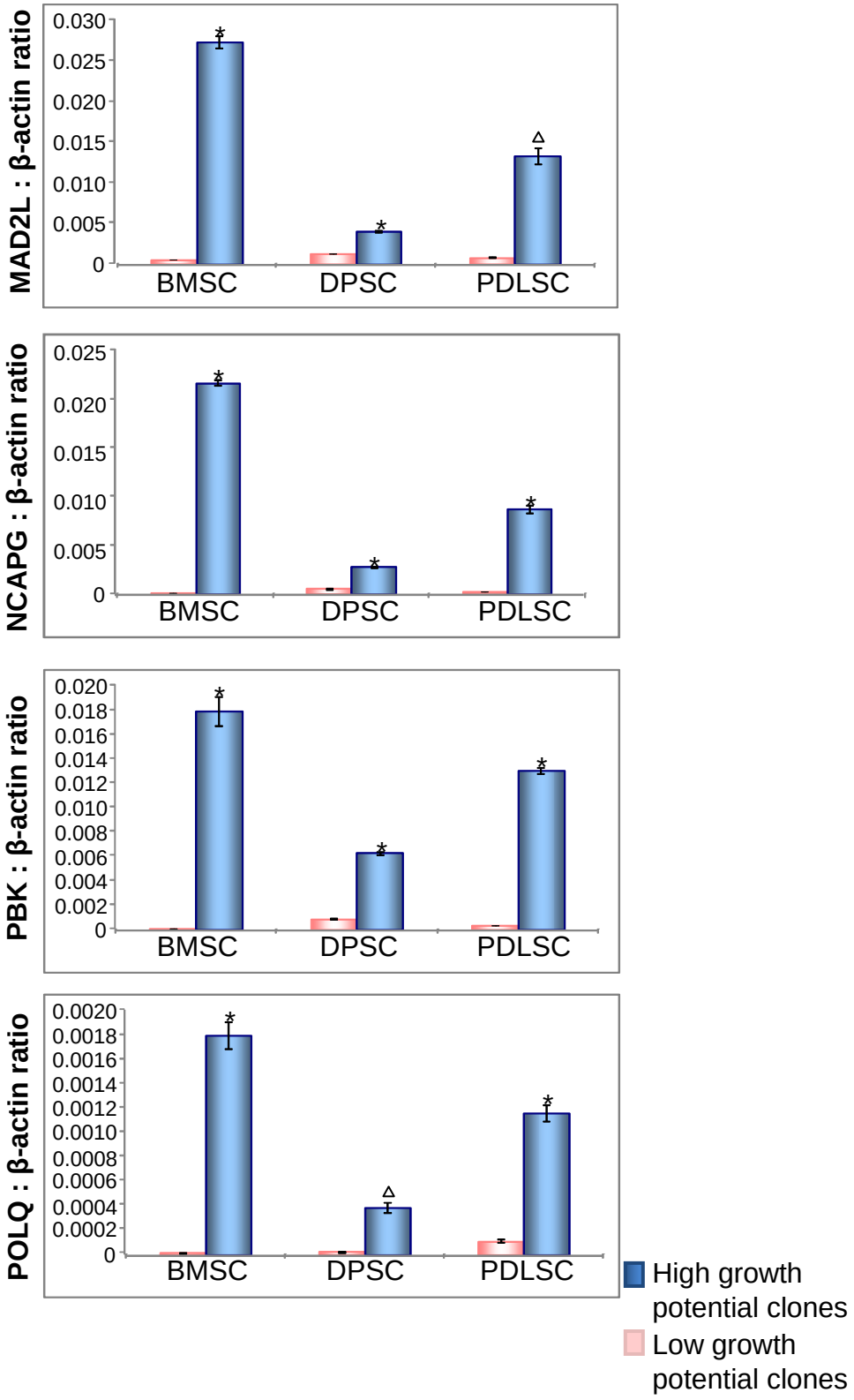
MAD2L : β-actin ratio
0.030
0.025
0.020
0.015
0.010
0.005
0
BMSC
DPSC
PDLSC
NCAPG : β-actin ratio
0.025
0.020
0.015
0.010
0.005
0
BMSC
DPSC
PDLSC
PBK : β-actin ratio
0.020
0.018
0.016
0.014
0.012
0.010
0.008
0.006
0.004
0.002
0
BMSC
DPSC
PDLSC
POLQ : β-actin ratio
0.0020
0.0018
0.0016
0.0014
0.0012
0.0010
0.0008
0.0006
0.0004
0.0002
0
BMSC
DPSC
PDLSC
High growth potential clones
Low growth potential clones

Figure 4.12 Confirmation of RPA3, RRM2, TOP2A and UBE2C Expression by Real-Time PCR.

Representative graphs of Real-Time PCR analysis of expression levels of differentially expressed genes, RPA3, RRM2, TOP2A and UBE2C, confirm up-regulation of these genes in high growth/multi-differentiation potential clones in comparison to low growth potential clones. The data represent the mean values ± standard deviations of triplicate experiments normalized to the house keeping β-actin gene. Statistical significance of and (*) $p<0.0001$ was determined using the unpaired student t-test.

Figure 4.12

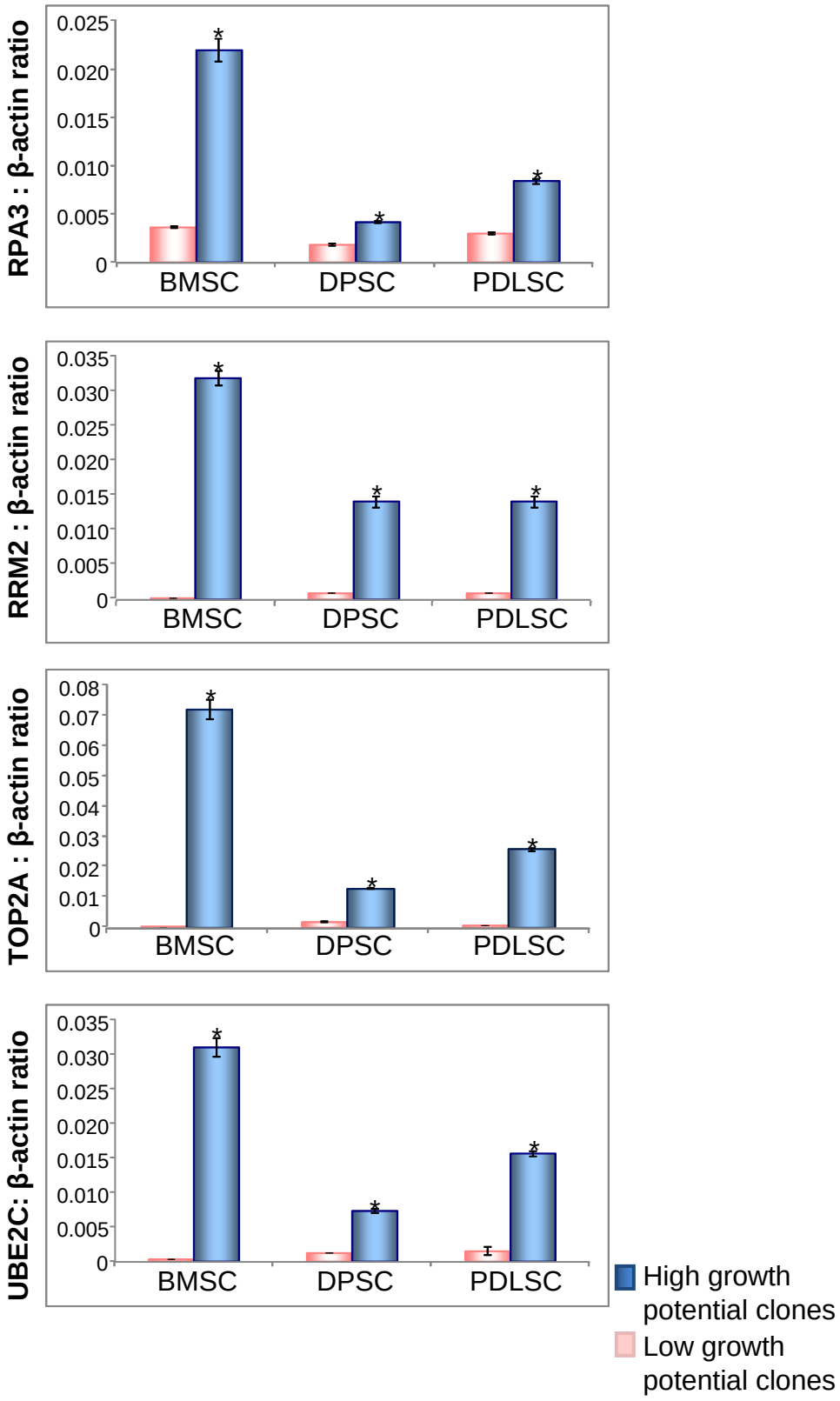
RPA3 : β-actin ratio
0.025
0.020
0.015
0.010
0.005
0
BMSC
DPSC
PDLSC
RRM2 : β-actin ratio
0.035
0.030
0.025
0.020
0.015
0.010
0.005
0
BMSC
DPSC
PDLSC
TOP2A : β-actin ratio
0.08
0.07
0.06
0.05
0.04
0.03
0.02
0.01
0
BMSC
DPSC
PDLSC
UBE2C: β-actin ratio
0.035
0.030
0.025
0.020
0.015
0.010
0.005
0
BMSC
DPSC
PDLSC
High growth potential clones
Low growth potential clones

Figure 4.13 Comparison of Gene Expression Levels for E2F-2, LDB-2, PTTG-1 and TWIST-1 in BMSCs, PDLSCs, DPSCs and HFFs.

Representative graphs of Real-Time PCR analysis showing expression levels of regulators of transcription E2F-2, LDB-2, PTTG-1 and TWIST-1 in high growth/multi-differentiation potential BMSC, DPSC and PDLSC clones in comparison to HFFs. The data represent the mean values ± standard deviations of triplicate experiments normalized to the house keeping gene, β-actin. Statistical significance of (*) $p<0.01$ was determined using the unpaired student t-test.

Figure 4.13

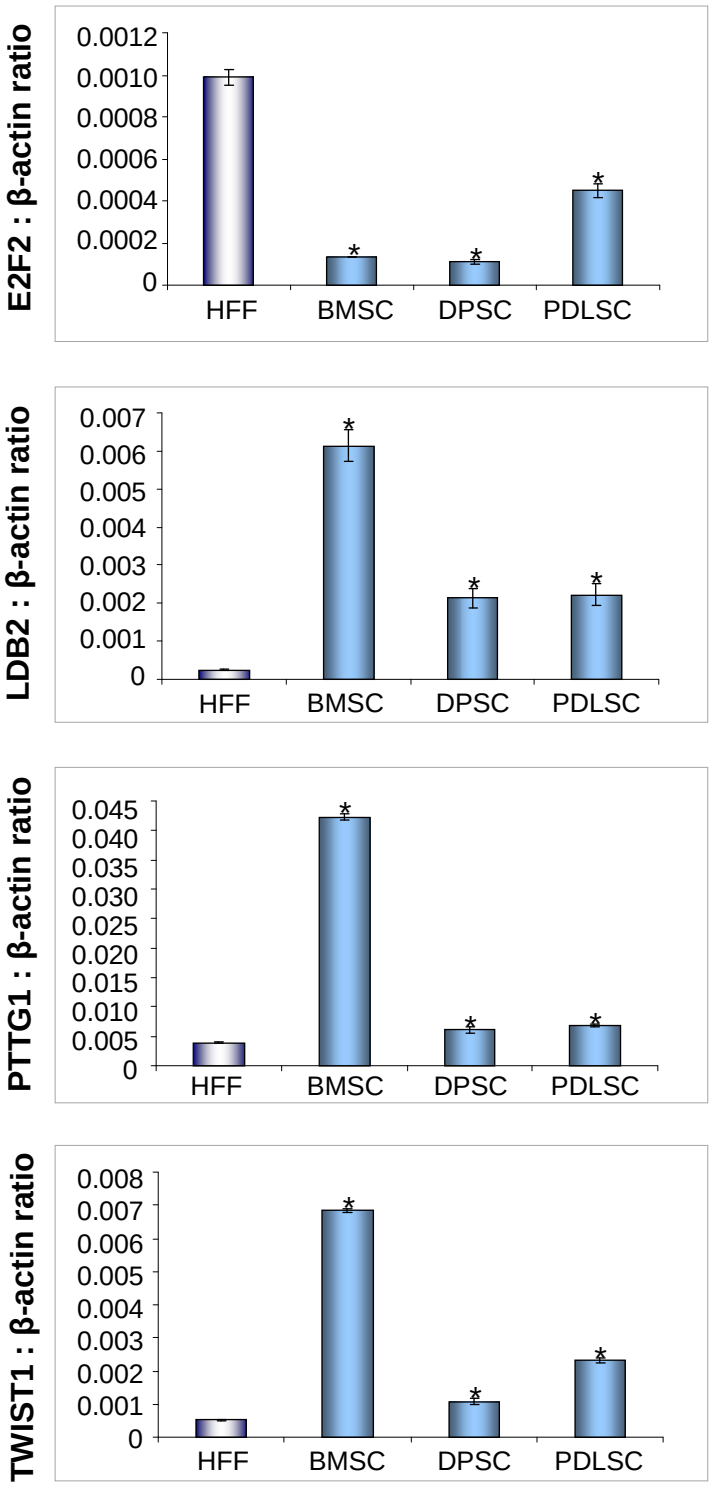
E2F2 : β-actin ratio
0.0012
0.0010
0.0008
0.0006
0.0004
0.0002
0
HFF
BMSC
DPSC
PDLSC
LDB2 : β-actin ratio
0.007
0.006
0.005
0.004
0.003
0.002
0.001
0
HFF
BMSC
DPSC
PDLSC
PTTG1 : β-actin ratio
0.045
0.040
0.035
0.030
0.025
0.020
0.015
0.010
0.005
0
HFF
BMSC
DPSC
PDLSC
TWIST1 : β-actin ratio
0.008
0.007
0.006
0.005
0.004
0.003
0.002
0.001
0
HFF
BMSC
DPSC
PDLSC

The data in **Figures 4.7–4.13** represent the mean values ± standard deviations of triplicate experiments normalised to the house keeping β-actin gene. Statistical significance was determined using the unpaired t-test.

4.2. DISCUSSION

4.2.1. Comparison of Affymetrix® U133 and Illumina® WG-6 Microarray Platforms in Gene Expression Profiling of Clonal Lines of PDLSCs

Gene expression profiling using microarray technology allows for the assessment of levels of expression of genes across numerous biological samples where the variations may account for the phenotypic/functional differences present in those samples. The advantage of whole genome arrays is the broad evaluation of gene expression patterns, where a number of genes act in a coordinated manner revealing involvement of specific pathways and connections between pathways, as such novel genes can be identified or an unsuspected pathway involvement can be determined [271].

In a pilot study we compared the gene expression patterns of PDLSC clones of high growth/multi-differentiation potential and low growth potential across both Illumina and Affymetrix designed platforms. We identified similar numbers of differentially expressed genes between the different PDLSC clones tested using both microarray technologies. Further analysis of the data found that approximately 40% of the differentially expressed genes were common to both the Illumina and Affymetrix microarrays. In the absence of any clear distinctions between the two microarray technologies, the Illumina® WG-6 platform was chosen for subsequent gene expression profiling studies based on the convenience of the BeadChip® technology for parallel interrogation of six RNA samples in order to generate individual data sets that could be further treated and manipulated independently for each of the samples tested, as previously described [274].

4.2.2. Identification of Gene Sets Expressed by Long Lived, Multi-Potential BMSC, DPSC and PDLSC Clonal Lines

Numerous studies have focused on characterising gene expression profiles of MSCs in an attempt to identify specific genes associated with maintenance of features of stemness, as summarised in a recently published review [275]. A recent publication has reported on the

gene expression profiling of bone marrow derived MSCs at a clonal level where expression patterns of stem cell pathway related genes were compared between fast growing/tri-potential differentiation capacity and slow growing/uni-potential differentiation capacity BMSC clones [245]. In this study a macro-array platform representing 84 stem cell pathway genes identified 10 genes that were upregulated in fast-growing clones (**Table 4.2**). The values presented in the table represent fold changes of gene expression in fast-growing clones. These genes are associated with maintenance of self renewal and lineage determining factors in numerous cell types, including MSCs [245]. Similarly, the aim of this study was to gain insight into molecular mechanisms that govern MSC renewal and differentiation capacity. In contrast, the present study used a whole genome array to assess gene expression profiles of clones exhibiting functional differences across MSC populations derived from three stromal tissues.

Assessment of gene expression profiles comparing cells of low and high growth capacity and varied differentiation potential within the BMSC, DPSC and PDLSC populations resulted in the identification of differentially expressed gene sets for each of the tissue types. Bioinformatic interrogation of the microarray data sets identified several hundred differentially expressed genes associated with high growth/multi-differentiation potential clonal populations. Further cross-comparative analyses of the differential gene expression patterns across all three stromal tissues identified 24 differentially expressed genes common to high growth/multi-differentiation potential BMSCs, DPSCs and PDLSCs, which were confirmed by real time PCR. As anticipated, a large proportion of these genes have been reported to be involved in cell cycle, cell division and mitosis, as well as in other cellular processes including DNA repair and replication and cellular differentiation. Furthermore, common to the findings of the study by Mareddy and colleagues [245] discussed earlier, we identified CDC2 to be associated with BMSCs of high growth potential. We further confirmed the upregulation of this gene in highly proliferative DPSC and PDLSC populations. Interestingly, a small subset of the common MSC-like genes were found to be well characterised transcription factors (E2F-2, PTTG-1 and TWIST-1), and a transcriptional co-factor (LDB-2).

To confirm that the identified transcription factors are specific to isolated MSC populations and are not potentially upregulated in any cell type of high proliferative potential we further assessed their expression in highly proliferating HFFs that lack the

Table 4.2 A List of Up-Regulated Genes in Fast Growing BMSC Clones of Tri-Potential Differentiation Capacity [245].

NOTE:
This table is included in the print copy of the thesis held in the University of Adelaide Library.

ability to form mineralised tissue or fat [55]. As E2F family members play a major role in regulating cellular proliferation, we expected and confirmed high expression of E2F-2 in high proliferative HFFs. In contrast, higher levels of LDB-2, PTTG-1 and TWIST-1 expression were observed in MSC-like cells in comparison to HFF. Although the role played by these transcriptional regulators in the maintenance of high growth/multi-differentiation potential MSC remains to be determined, recent studies suggest that E2F-2, PTTG-1 and TWIST-1 may play critical roles in BMSC growth and development.

Previous studies have shown that the transcription factors of the E2F family regulate cellular proliferation by controlling the transcription of numerous genes involved in DNA replication, DNA repair, mitosis and cell cycle progression [276-281]. This family of genes can be subdivided into two main groups, including repressors and activators of E2Fs. E2F-2 together with E2F-3a is a potent activator that transiently binds and activates E2F target promoters [276-281]. While the specific role of E2F-2 in cell growth still remains to be fully elucidated a study by Won *et al* investigated the role of E2F transcription factors in transcriptional repression of human telomerase reverse transcriptase (hTERT) gene [282]. Telomeres are specialized structures, vital to maintenance of chromosomal stability, located at the ends of chromosomes. They prevent attrition, end-to-end fusion and chromosomal rearrangements. Telomerase is an enzyme complex essential to preservation of the length of telomeres in rapidly dividing cells [283-285]. This enzyme adds telomeric DNA repeats at the ends of newly duplicated telomeres and as such preserves their length throughout replication cycles and protects the chromosome from degradation [286]. hTERT is the catalytic subunit of telomerase and plays an important role in telomerase elongation [283, 285, 287]. Interestingly, studies from Won and colleagues suggest that E2F-1, E2F-2 and E2F-3 activate hTERT in normal somatic cells suggesting that activation of E2F-2 in high proliferative MSC clones may maintain expression levels of hTERT and, hence telomerase activity [282]. Recent work by Infante *et al* investigated the role of E2F-2 in cell proliferation by studying the response of T cells in terms of the kinetics of cell cycle entry and cell proliferation when stimulated with activating antibody (CD3) in E2F-2 knockout mice [288]. These studies confirmed previous findings by showing that E2F-2 normally plays a negative role to restrain cell cycle progression [288-290, 291]. Further findings indicate that E2F-2 is a negative regulator of the expression of genes required for cell cycle regulation, mitosis, DNA metabolism and repair, as loss of E2F-2, in resting T cells, led to an upregulation of such

genes including MCM-2, MCM-6, CDC-6, CYCA, CYCB, CDC2A and CHK-1 [288]. Past research has shown that E2F-2 can promote terminal differentiation and irreversible cell cycle exit of neurotrophin dependent sympathetic neurons [292] as well as promoting cell cycle check point control to prevent damage during terminal erythroid differentiation [293]. Recent work by Ebelt and colleagues shows that overexpression of E2F-2 has the potential to induce hypertrophic cell growth as well as proliferation of terminally differentiated cardiomyocytes in adult mouse heart [294].

LIM domain-containing proteins play a vital role during embryogenesis as they constitute regulators and determinants of cellular fate and differentiation [295]. The LIM domain is a zinc finger motif found in a diverse set of proteins, including transcription factors of the LIM-homeodomain (LIM-HD) and LIM-only (LIM-O) protein families [296, 297]. LIM domains have been shown to mediate protein-protein interactions of pivotal importance in vertebrate development and cellular differentiation [295, 296, 298-300]. Loss of function or incorrect expression of LIM-HD transcription factors results in severe biological consequences, highlighting the importance of these genes in development [298, 301, 302]. LIM domain binding protein, LDB family, also referred to as Clim (Co-factor of LIM domains) was originally identified as a co-activator of LIM-HD and LMO transcription factors [287, 297, 303-305]. Interaction of LIM-HD and LDB is thought to be critical for the exertion of transcriptional and biological activity of these developmental regulators [287, 306-311]. LDB-2, one of the proteins within the LDB family [312], binds the LIM domain of LIM-HD and LMO proteins [313]. It is believed that the function of LIM domain binding proteins is to recruit LDB factors to enhance transcription of target genes [297]. It has been shown that association of LDB factors to LIM-HD proteins is vital to development of specific cell populations in the spinal cord including inter-neurons and motor-neurons during neural tube development [312, 314]. It was further reported that cellular protein concentration of LDB is a critical determinant of LIM-HD activity *in vivo* [312, 315]. Recently, it was found that the expression of LDB-2 is significantly reduced in gangliomas. Fassunke *et al* used *in situ* hybridization to determine that the reduced expression was localised to dysplastic, clustered neuronal components but not in glial cell elements of gangliomas [313]. They observed that neurons with reduced levels of LDB-2 exhibit an altered morphological phenotype and were the first to report on this association of LDB-2 with molecular mechanisms underlying impaired development of a regular cortical architecture [313]. Therefore the lack of LDB-2 in developing neurons may affect

neuronal migration and differentiation processes and may result in the development of an abnormal neuronal network [313].

Pituitary tumor-transforming gene 1 (PTTG-1) was originally isolated from rat pituitary cells [316] and was termed Securin upon its latter discovery in humans [317]. This transcription factor is involved in many cellular processes including mitosis, cell cycle progression, DNA repair and maintenance of chromosome stability [317-320]. PTTG-1 exerts its actions as an inhibitor of sister-chromatid separation, by binding and inactivating Separase, a protease that cleaves the Scc1 cohesin subunit responsible for sister chromatid adhesion at the metaphase to anaphase transition [317]. Due to its role in chromosomal aggregation, the upregulation of PTTG-1 leads to chromosomal misaggregation and hence genomic imbalance. These events account for the oncogenic potential of upregulated PTTG-1 expression, which has been associated with a variety of endocrine related tumors (pituitary, thyroid, breast, ovarian and uterine) and non-endocrine related cancers (central nervous system, pulmonary system and gastrointestinal system) [321-328]. An additional mechanism potentially accounting for tumorigenesis of PTTG-1 is the formation of positive feedback loop with fibroblast growth factor (FGF) to stimulate tumour angiogenesis [320, 329, 330]. As such PTTG-1 has been termed an oncogene and a prognostic marker of numerous cancers. Whilst the role of PTTG-1 does not appear to be critical for normal foetal development, mouse embryonic fibroblasts that lack PTTG-1 expression grow abnormally in culture, even though PTTG-1 null mice are essentially normal [331]. However, a role for this gene in postnatal BMSC maintenance and proliferation has recently been proposed in studies where PTTG-1 deletion lead to a decrease in BMSC proliferation *in vitro* and was associated with increased sensitivity to hypoxia and cellular senescence [332].

TWIST-1 is a basic helix-loop-helix (bHLH) containing transcription factor [333-336] found to be crucial for correct patterning of the skeleton [334, 336, 337, 338], where it is down regulated during endochondral and intramembranous fetal bone development [339]. The expression of TWIST-1 appears greatest at sites of immature bone cells and decreases in more mature bone cell populations during calvaria and suture development [340, 341]. The importance of TWIST-1 in bone development is highlighted both in mice and humans where TWIST-1 heterozygosity leads to premature osteoblast differentiation and cranial suture fusion in the skull. These abnormalities result in craniosynostosis (Saethre-Chotzen

syndrome), a condition which is often associated with dysmorphic facial findings and various limb abnormalities [342-344]. Studies using double murine heterozygotes containing TWIST-1/RUNX-2 or DERMO-1/RUNX-2 deletions, showed that both TWIST-1 and DERMO-1 (TWIST-2) negatively regulate RUNX-2 induced bone formation during murine development [342]. Previous studies have reported that TWIST-1 expression can be identified in different murine osteoblastic cell lines, and that this bHLH gene is down-regulated during osteogenic differentiation *in vitro* [339, 342, 345-347]. Furthermore, work by Glackin and colleagues has shown a reduced capacity of osteosarcoma cell lines to undergo osteoblastic maturation as a result of enforced expression of either TWIST-1 or DERMO-1, whereas an increase in bone cell maturation was observed due to overexpression of TWIST-1 or DERMO-1 antisense, in these cell lines [334, 336]. Recent work in our laboratory has identified a potential role for both TWIST-1 and DERMO-1 in BMSC proliferation potential and adipogenic commitment while inhibiting osteo/chondrogenic development [230].

The present study suggests that a coordinated action of numerous genes is involved in control of multiple signalling pathways which in turn regulate proliferation and differentiation of MSCs. Collectively, the findings implicate E2F-2, LDB-2, PTTG-1, and TWIST-1 as potential key molecules that mediate maintenance, growth and development of mesenchymal stem-like cells derived from different anatomical sites. Whilst the significance of these transcriptional factors is mostly speculative, recent work in our laboratory has identified a potential role for TWIST-1 in MSC growth and commitment [230] and this role is further investigated in the following chapter.

Chapter 5:

The Effect of Induced TWIST-1 Expression on MSC Growth and Commitment

5. The Effect of Induced TWIST-1 Expression on MSC Growth and Commitment

Our gene expression profiling study (**Chapter 4**) found that TWIST-1 expression was elevated in highly proliferative and multi-potential BMSC, DPSC and PDLSC clones [177]. Moreover, recent work in our laboratory has shown that immature clonogenic BMSCs freshly isolated from human bone marrow aspirates express high levels of TWIST-1 which is rapidly down regulated following *ex vivo* expansion [230]. Further analyses identified a potential role for TWIST-1 in both BMSC growth and development. Enforced expression of TWIST-1 in culture expanded BMSCs increased their overall life-span while maintaining an immature genotype and phenotype. Interestingly, TWIST-1 over-expressing BMSCs demonstrated an enhanced capacity for adipogenic differentiation while inhibiting osteogenesis and to a lesser extent chondrogenic development [230]. Following on from this work, our microarray findings support the notion that TWIST-1 may act to support the self-renewal of different MSC populations whilst inhibiting maturation and calcified tissue formation.

5.1.1. The Role of TWIST-1 in Development

TWIST-1 was firstly identified by Nusslein-Volhard and was ascribed the role of dorsoventral patterning in *Drosophila*, critical for the onset of gastrulation and the formation of mesoderm [335, 348]. This evolutionary conserved member of the basic helix-loop-helix (bHLH) transcription factors is essential for the development of embryonic gastrulation, development of the mesoderm and crucial for correct patterning of the skeleton [335, 334, 336, 349, 337, 338].

Molecules within the bHLH family exert their effect by homo- or hetero- dimerizing with other molecules within this family and, through binding to a conserved E-box region on gene promoters, act to initiate/promote or inhibit transcription. These transcription factors play a key role in developmental process vital to cell survival, by recognition and binding to the E-box motifs [350]. Induction of expression of target genes can be achieved by increased affinity for the DNA binding site or by binding to novel DNA binding sites. Conversly, repression of activity mainly occurs through interactions with HLH proteins that lack the basic DNA binding domain or contain the residues that disrupt the helical structure in the domain [351]. TWIST-1 exhibits an intriguing ability to perform numerous

functions required by the cell and, due to this, is involved in a wide spectrum of process critical to cell survival, cell death and cell development.

In *Drosophila*, the loss of TWIST-1 expression, results in a lack of development of most mesodermally derived organs due to the failure of the mesoderm layer to develop in homozygous mutant embryos. As a result of abnormal head involution, the shape of the embryo appears 'twisted' in the egg [352]. During mouse embryonic development TWIST-1 transcripts are primarily detected in the anteriorlateral mesoderm, followed by expression in the head mesenchyme, branchial arches, somites, lateral plate mesoderm, allantoic stalk and other tissues [353]. A gene deletion study by Chen and Behringer assessed the role of TWIST-1 in mouse development and found it to be embryonicaly lethal, where TWIST-1 null mice died at embryonic day 11.5 presenting with vascular defects, head mesenchyme defects and failure of neural tube closure in the cranial region [333]. Moreover, TWIST-1 heterozygous mice, exhibited skull defects and limb abnormalities due to premature osteoblast differentiation and cranial suture fusion in the skull [354].

5.1.2. The Involvement of TWIST-1 in Seathre-Chotzen Syndrome

In humans, TWIST-1 mutations, within the highly conserved DNA binding and HLH domains, are displayed through an autosomal dominant syndrome (Saethre-Chotzen) where nonsense, missense, insertion and deletion mutations identified in TWIST-1 indicate its involvement in the pathogenesis of this syndrome [342-344, 355]. Saethre-Chotzen (SC), is one of the most common syndromes of craniosynostosis, a congenital disorder characterised by premature fusion of calvarial bones, hence abnormal craniofacial growth [355]. Following its initial description by Saethre and Chotzen, SC syndrome was described in greater detail by Pantke and colleagues in 1975 [356]. The major feature of SC syndrome is synostosis of coronal sutures with brachycepahly, whilst the degree and the time of onset varies between individuals. The most prominent phenotypic features include dysmorphic facial findings and limb abnormalities [355]. This is generally associated with raised intracranial pressure, impaired cerebral blood flow, airway obstruction, impaired vision and hearing, learning difficulties and adverse psychological effects [357-360]. Additionally, multiple dental anomalities, were identified in patients with syndromic and non syndromic craniosynostosis [361, 362]. The birth prevalence of SC syndrome is approximately 1 in 25 000 to 1 in 50 000 live births [355, 363].

5.1.3. The Role of TWIST-1 in Cellular Differentiation

TWIST-1 has been implicated in the inhibition of differentiation of cells of the osteogenic [334, 341, 346], chondrogenic [364]and myogenic lineages [364, 365]. The expression of TWIST-1 appears to be greatest at sites of immature bone cells and decreases in more mature bone cell populations during calvaria and suture development [340, 341]. Previous studies have reported that TWIST-1 expression can be identified in different murine osteoblastic cell lines, and that this bHLH gene is down-regulated during osteogenic differentiation and maturation *in vitro* [339, 342, 345-347]. Additionally, Lee *et al* have identified the potential role of TWIST-1 as a master regulator in initiation of bone cell differentiation [334]. They showed that in humans, TWIST-1 plays a regulatory role in differentiation of osteoblastic progenitors and influences morphology of bone cells. Enforced expression of TWIST-1 appeared to maintain cells in the early osteoprogenitor-like state inhibiting progress to further maturation [334]. Studies using double murine heterozygotes containing TWIST-1/RUNX-2 deletions, showed that TWIST-1 negatively regulated RUNX-2 induced bone formation during murine development [342]. They further clarified an important stage in bone formation by determining that this regulation occurs through direct interactions of TWIST box (carboxyl-terminal region of TWIST) and the Runt domain of RUNX-2, which prevents DNA binding and gene activation by RUNX-2 [342].

A few studies have examined the involvement of TWIST-1 in the development of dental tissues. Galler *et al* investigated its role in dental pulp homeostasis, and found that TWIST-1 plays a regulatory role in odontoblast differentiation [366]. Confirmatory to previous research, they found that TWIST-1 actions are closely linked and dependent on its interaction with RUNX-2. They found that TWIST-1 deficiency in mice affects precursor odontoblast-like cells, and results in premature differentiation and formation of the dentin matrix. Due to a decrease in TWIST-1 levels, odontoblast progenitor cells appeared to become more responsive to RUNX-2 and this resulted in deposition of pulp stone-like material within the core [366]. Additionally, TWIST-1, amongst other markers involved in neural crest cell differentiation, was found to be expressed in a novel population of progenitor cells derived from pad-like tissue located under the pulp of impacted third molars, termed dental neural crest-derived progenitor cells (dNC-PCs) [367]. A study by Komaki *et al* investigated the extent of TWIST-1 involvement in

osteoblastic differentiation of PDL derived cells. They found that Twist-1 was localised along alveolar bone surface in rat PDL, and that it was constitutively expressed in PDL cells. Their studies concluded that that repression of endogenous TWIST-1 levels stimulates osteoblastic differentiation [368].

Considering the previously demonstrated involvement of TWIST-1 in the formation of normal mineralised tissues, it is reasonable to suggest that TWIST-1 holds a fundamental part in growth and differentiation processes of MSCs derived from mineral forming tissues. In this study we assessed the effect of enforced TWIST-1 expression on cellular proliferation and differentiation potentials in MSC-like cells derived from dental pulp and periodontal ligament.

5.2. Results

5.2.1. Generation of DPSC and PDLSC Lines Over-Expressing TWIST-1

TWIST-1 is highly expressed by immature, multi-potential BMSCs, but is down-regulated by the majority of their progeny following culture expansion [230]. Similarly, we investigated the role of TWIST-1 during proliferation and differentiation of DPSC and PDLSC populations. Bulk preparations of cultured human DPSCs and PDLSCs at passage (P) 2 were used for the transduction studies. To determine the effect of TWIST-1 on DPSC and PDLSC growth and development, TWIST-1 over-expressing DPSC and PDLSC lines were generated by retroviral transduction and selected based on GFP expression using FACS. Transduction efficiency was demonstrated in all of the assessed TWIST-1 over-expressing DPSC and PDLSC populations (**Figure 5.1A**). The median and range values of GFP expression for TWIST-1 over-expressing cells and vector controls, prior to and post sorting are displayed in **Table 5.1**.

Figure 5.1 Enforcement of TWIST-1 Expression in DPSC and PDLSC Populations

DPSC and PDLSC lines were stably transduced with pRUFeGFP construct containing TWIST-1 cDNA or vector alone (GFP). (**A**) Representative micrographs demonstrate the transduction efficiency of TWIST-1 overexpressing (**i**) (scale bar = 200μ) and (**iii**) (scale bar = 50μ) DPSC lines and (**ii**) (scale bar = 200μ) and (**iv**) (scale bar = 50μ) PDLSC lines. (**B**) Real-Time PCR analysis demonstrated increased levels of expression of TWIST-1 in overexpressing (**i**) DPSC and (**ii**) PDLSC lines in comparison to vector controls. The data represent the mean values ± standard deviations of triplicate experiments normalized to the house keeping β-actin gene. Statistical significance of (*) of $p<0.001$ was determined by the unpaired t-test. (**C**) Representative immunoblots show increased levels of TWIST-1 protein expression (~28kD) in high expressing TWIST-1 (**i**) DPSC lines and (**ii**) PDLSC lines in comparison to GFP vector controls. Membranes were further probed with anti-HSP90 (~90kD) to confirm equal protein loading.

Figure 5.1

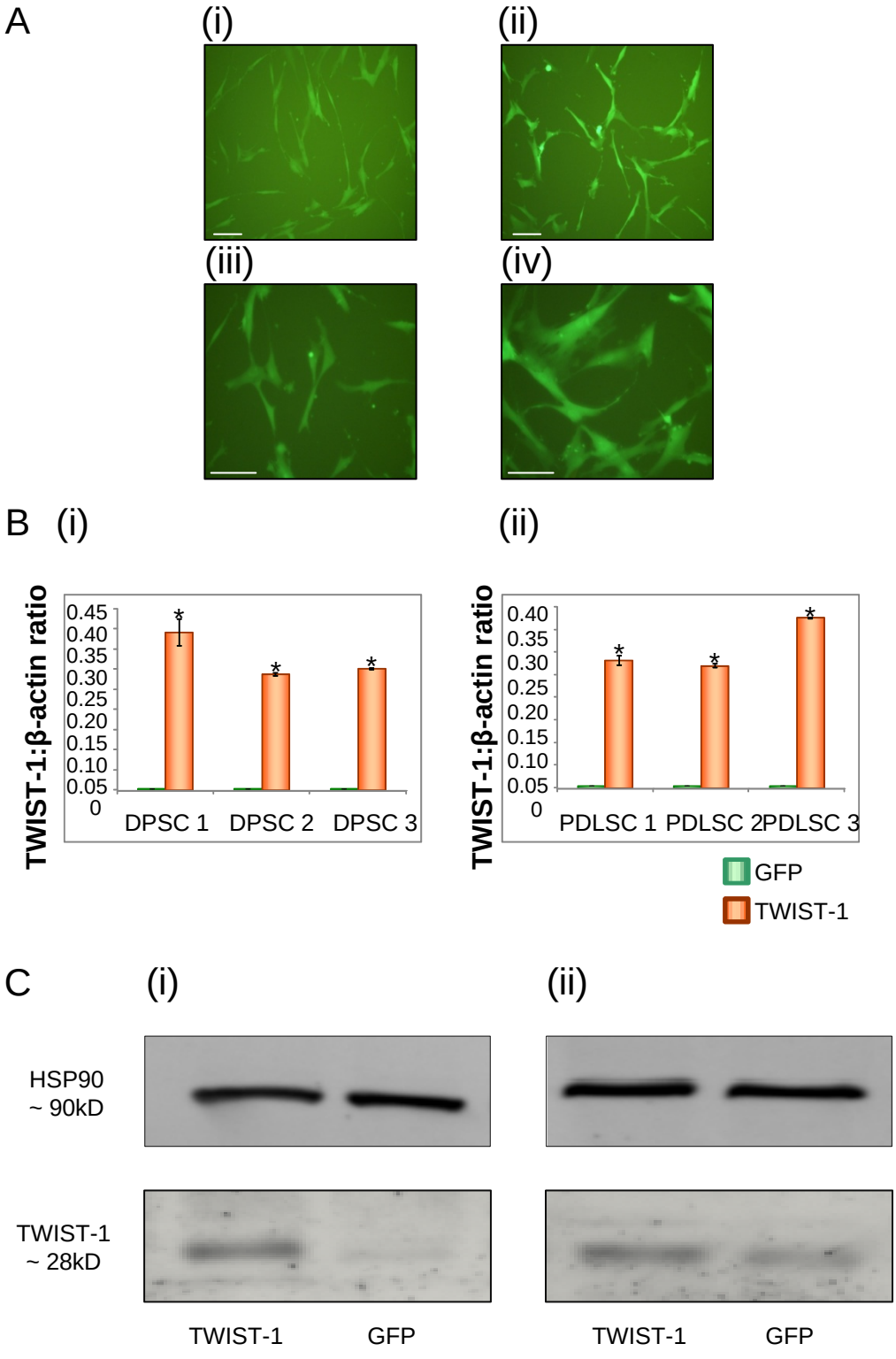
A
(i)
(ii)
(iii)
(iv)
B (i)
(ii)
TWIST-1:β-actin ratio
0.45
0.40
0.35
0.30
0.25
0.20
0.15
0.10
0.05
0
DPSC 1
DPSC 2
DPSC 3
TWIST-1:β-actin ratio
0.40
0.35
0.30
0.25
0.20
0.15
0.10
0.05
0
PDLSC 1
PDLSC 2
PDLSC 3
GFP
TWIST-1
C
(i)
(ii)
HSP90
~ 90kD
TWIST-1
~ 28kD
TWIST-1
GFP
TWIST-1
GFP

Table 5.1 Levels of GFP Expression for TWIST-1 Over-Expressing DPSC and PDLSC Populations and Vector Controls.

	pre-sorting		post-sorting	
	Median (%)	Range (%)	Median (%)	Range (%)
DPSC				
GFP	40.6	39.2 -68.6	88.3	83.9 - 97.8
TWIST	35.8	32.9 - 59.8	90.9	86.7 - 94.8
PDLSC				
GFP	43.4	26.2 - 50.0	93.1	84.9 - 97.0
TWIST	35	22.8 - 41.2	92.6	84.0 - 95.3

Real-time PCR analysis identified increased levels of TWIST-1 expression in over-expressing DPSC and PDLSC populations compared to vector controls. Statistical significance (*) of $p<0.001$ was determined by the unpaired t-test (**Figure 5.1B**). Accordingly, increased levels of Twist-1 protein were identified in high expressing TWIST-1 MSC populations (Figure 5.1C).

5.2.1.1. The Role of TWIST-1 in Cellular Proliferation Potential of DPSCs and PDLSCs

Assessment of DNA synthesis was used as a surrogate marker for the rate of cellular proliferation in TWIST-1 over-expressing cells and vector controls. DPSCs and PDLSCs were labelled with BrdU, which is incorporated into the DNA during the S phase of cycling cells. Hence, the measured amount of incorporated BrdU is directly related to the rate of cell division. The concentration of BrdU in proliferating DPSCs and PDLSCs was measured at 5 days of culture. These findings demonstrated increased levels of BrdU in TWIST-1 over-expressing DPSC and PDLSC lines, indicative of higher rates of cellular proliferation in these cell populations in comparison to vector controls (statistical significance (*) of $p<0.05$ was determined by the unpaired t-test, n=3) (**Figure 5.2A and 5.3A**).

In parallel experiments, Wst-1 assays were used to measure metabolic activity of DPSC and PDLSC populations and as such assess the viability of these cells at 5 days of culture.

Figure 5.2 Enforced TWIST-1 Expression Promotes Proliferation Rate in DPSC Populations

Cellular proliferation rate was assessed using BrdU incorporation and WST-1 proliferation assays. Representative histograms show the rate of proliferation measured by (**A**) BrdU incorporation and (**B**) WST-1 concentration in Passage 2 TWIST-1 over-expressing DPSC lines and vector controls post selection, following five days of culture. Statistical significance of (*) of $p<0.05$ was determined between three TWIST-1 and three vector control DPSC populations by the unpaired t-test.

Figure 5.2

A

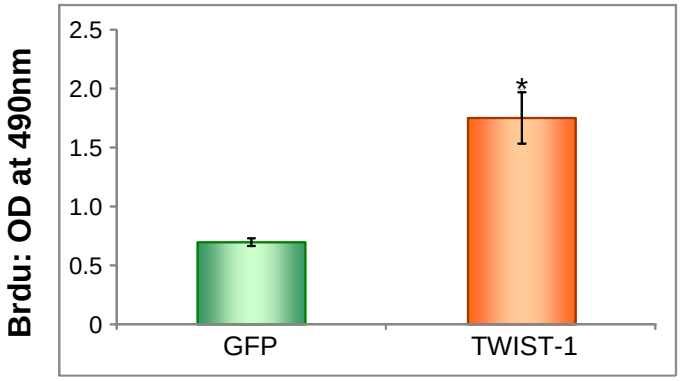
Brdu: OD at 490nm
2.5
2.0
1.5
1.0
0.5
0
*
GFP
TWIST-1

B

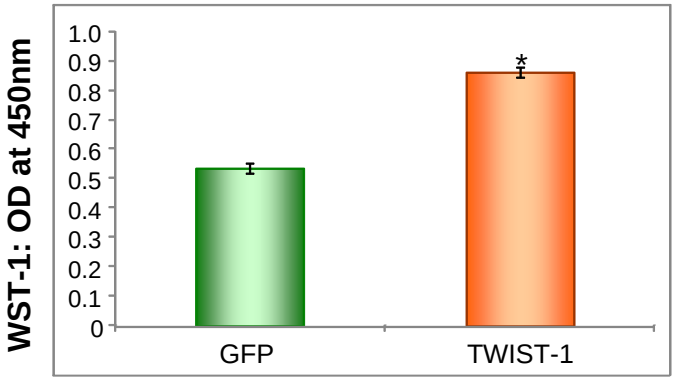
WST-1: OD at 450nm
1.0
0.9
0.8
0.7
0.6
0.5
0.4
0.3
0.2
0.1
0
*
GFP
TWIST-1


GFP
TWIST-1

Figure 5.3 Enforced TWIST-1 Expression Promotes Proliferation Rate in PDLSC Populations

Cellular proliferation rate was assessed using BrdU incorporation and WST-1 proliferation assays. Representative histograms show the rate of proliferation measured by (**A**) BrdU incorporation and (**B**) WST-1 concentration in passage 2 TWIST-1 overexpressing PDLSC lines and vector controls post selection, following five days of culture. Statistical significance of (*) of $p<0.05$ was determined between three TWIST-1 over-expressing and three vector control PDLSC populations by the unpaired t-test.

Figure 5.3

A

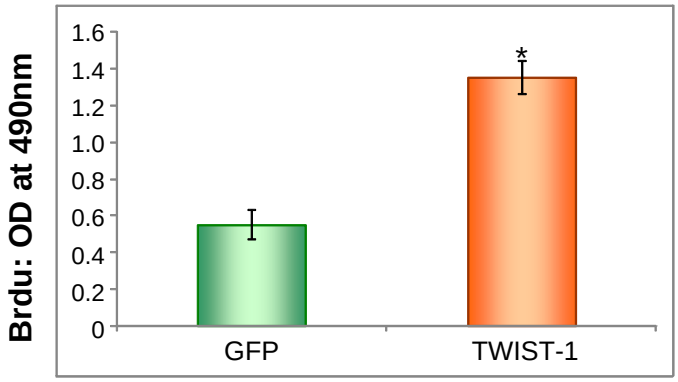
Brdu: OD at 490nm
1.6
1.4
1.2
1.0
0.8
0.6
0.4
0.2
0
*
GFP
TWIST-1

B

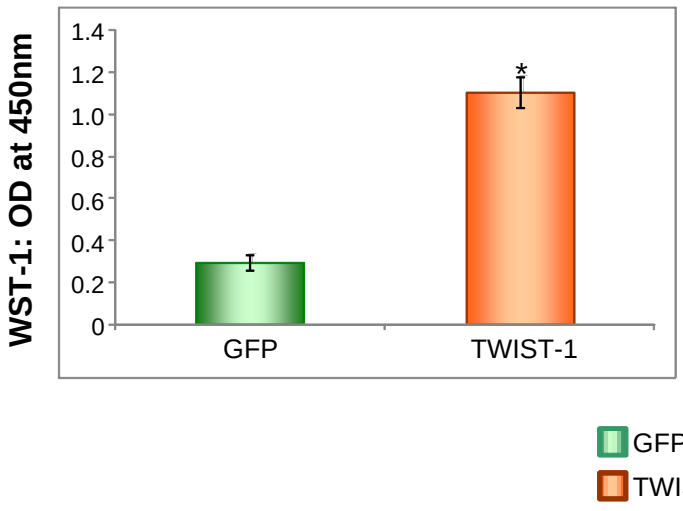
WST-1: OD at 450nm
1.4
1.2
1.0
0.8
0.6
0.4
0.2
0
*
GFP
TWIST-1
GFP
TWIST-1

These results displayed increased activity of mitochondrial dehydrogenase in TWIST-1 over-expressing DPSC and PDLSC lines, indicative of higher metabolic activity and viability of these cell populations in comparison to vector controls (statistical significance (*) of $p<0.05$ was determined by the unpaired t-test, n=3) (**Figure 5.2B and 5.3B**).

To assess the effect of enforced TWIST-1 expression on the growth potential and lifespan of DPSCs and PDLSCs, cumulative cell numbers and total population doubling values were determined using the formula ($\log_2$ final cell number/ $\log_2$ seeding cell number). In these experiments TWIST-1 over-expressing populations of DPSC and PDLSC and their vector controls generated from three different donors were expanded in continuous subculture until cellular senescence was achieved. The results of cumulative cell numbers (**Figure 5.4**) and population doublings (**Figure 5.5**) showed that TWIST-1 expression enhanced the rate of proliferation and appeared to prolong the lifespan in these MSC populations but were not found to be statistically significant (mean values ± standard deviation, n=3).

5.2.1.2. The Role of TWIST-1 in Cellular Differentiation Potential of DPSCs and PDLSCs

Assessment of differentiation potential was performed following osteogenic and adipogenic induction of P2 TWIST-1 over-expressing DPSC and PDLSC bulk populations and their vector controls generated from three different donors, by measuring the levels of mineral and lipid production, respectively. As enforced expression of TWIST-1 appeared to have a less pronounced effect on chondrogenic differentiation potential, in comparison to osteogenic and adipogenic potentials, in BMSCs [230] chondrogenic induction was not assessed for the TWIST-1 over-expressing DPSC and PDLSC populations.

In contrast to BMSC, the capacity of DPSCs to undergo osteogenic differentiation was enhanced in TWIST-1 over-expressing DPSC populations, compared to corresponding vector controls. This was manifested through their increased capacity to produce Alizarin Red staining mineralized nodules (**Figure 5.6A**) and an increase in calcium concentration measured within the extracellular matrix of these populations compared to vector controls, relative to non-induced control cultures. The data represent the mean values ± standard deviations generated from TWIST-1 over-expressing DPSCs and vector controls from three donors. Statistical significance of (*) of $p<0.05$ was determined by the unpaired t-test

Figure 5.4 Enforced TWIST-1 Expression Promotes Cellular Growth in DPSC and PDLSC Populations

The line graphs show cumulative cell number over successive cell passages until senescence was reached for (**A**) TWIST-1 over-expressing DPSCs and vector controls and (**B**) TWIST-1 over-expressing PDLSCs and vector controls. The data represent the mean values ± standard deviations of three TWIST-1 over-expressing and three vector control DPSC and PDLSC populations.

Figure 5.4

A

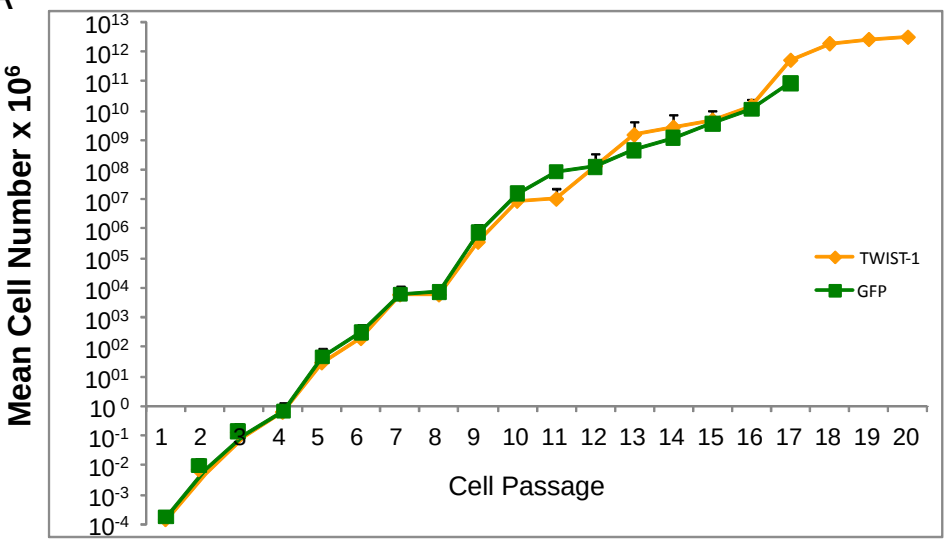
Mean Cell Number x 10⁶
10¹³
10¹²
10¹¹
10¹⁰
10⁰⁹
10⁰⁸
10⁰⁷
10⁰⁶
10⁰⁵
10⁰⁴
10⁰³
10⁰²
10⁰¹
10⁰
10⁻¹
10⁻²
10⁻³
10⁻⁴
1 2 3 4 5 6 7 8 9 10 11 12 13 14 15 16 17 18 19 20
Cell Passage
TWIST-1
GFP

B

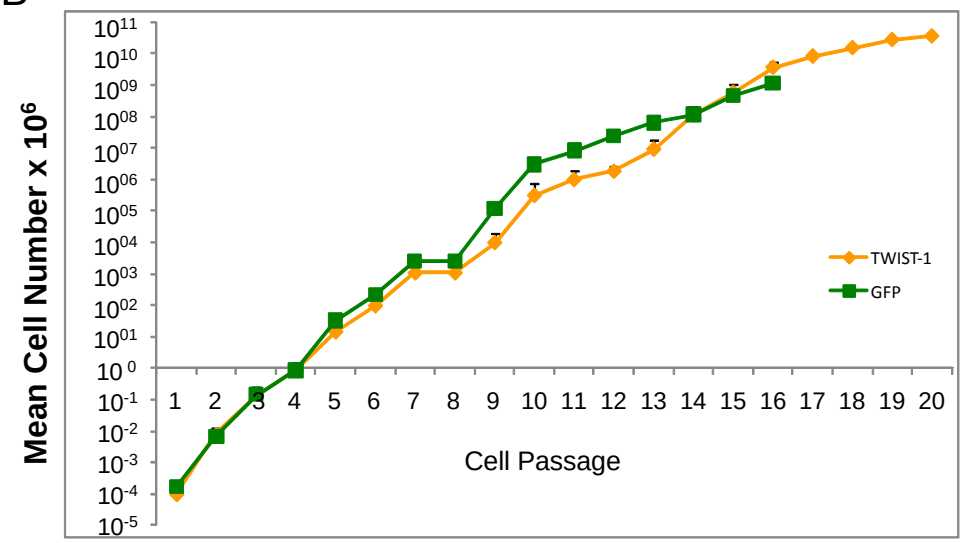
Mean Cell Number x 10⁶
10¹¹
10¹⁰
10⁰⁹
10⁰⁸
10⁰⁷
10⁰⁶
10⁰⁵
10⁰⁴
10⁰³
10⁰²
10⁰¹
10⁰
10⁻¹
10⁻²
10⁻³
10⁻⁴
10⁻⁵
1 2 3 4 5 6 7 8 9 10 11 12 13 14 15 16 17 18 19 20
Cell Passage
TWIST-1
GFP

Figure 5.5 Enforced TWIST-1 Expression Promotes Cellular Growth in DPSC and PDLSC Populations

The bar graphs show population doubling (PD) values for (**A**) TWIST-1 over-expressing DPSCs and vector control cell lines and (**B**) TWIST-1 over-expressing PDLSCs and vector control cell lines at the time of senescence. The data represent the mean values ± standard deviations of three TWIST-1 over-expressing and three vector control DPSC and PDLSC populations.

Figure 5.5

A

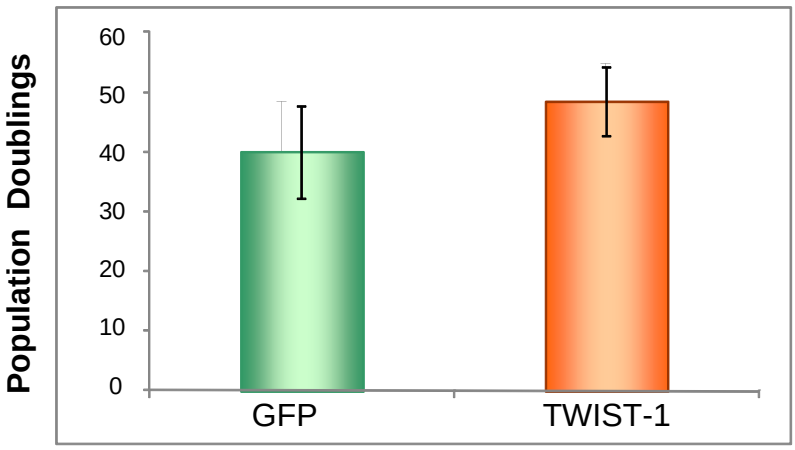
Population Doublings
60
50
40
30
20
10
0
GFP
TWIST-1

B

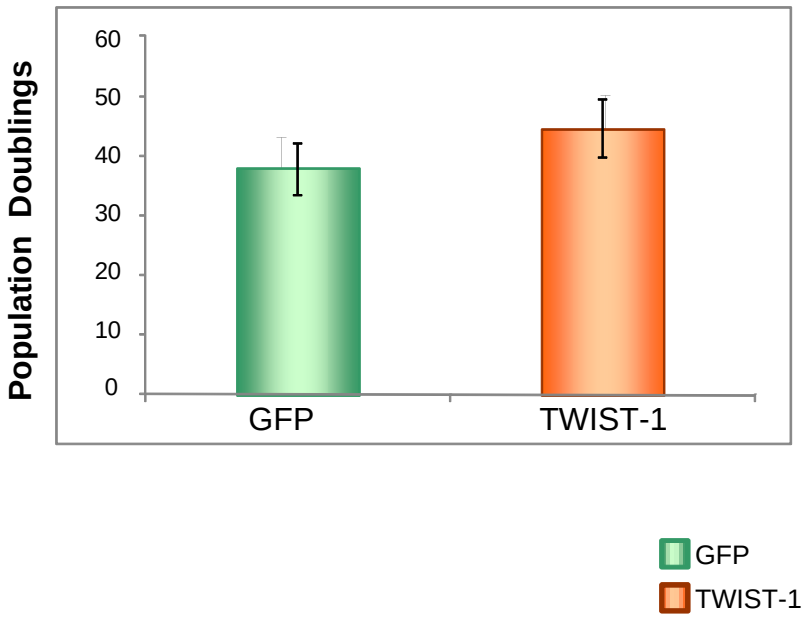
Population Doublings
60
50
40
30
20
10
0
GFP
TWIST-1
GFP
TWIST-1

Figure 5.6 Enforced TWIST-1 Expression Promotes Osteogenic Differentiation of DPSC

All of the TWIST-1 over-expressing DPSC lines showed an increased potential to form mineral in comparison to the vector controls. The presence of mineral nodules was identified by Alizarin Red staining (**A**) (scale bar = 200μm) of (**i**) vector controls and (**ii**) TWIST-1 over-expressing DPSCs, cultured under inductive osteogenic conditions. (**B**) Calcium concentration within the extracellular matrix was measured and normalised to DNA content per well. The data represent values of fold change ± standard deviation of TWIST-1 over-expressing DPSCs in comparison to the vector controls. (**C**) Real-Time PCR analysis demonstrated increased levels of expression of markers of osteogenesis, BMP, BSP, OPN and RUNX-2 in TWIST-1 over-expressing DPSC lines in comparison to the vector controls, relative to non-induced control cultures. The data represent the mean values ± standard deviations of triplicate experiments normalized to the house keeping β-actin gene. Statistical significance of (*) of $p<0.001$ was determined by the unpaired t-test.

Figure 5.6

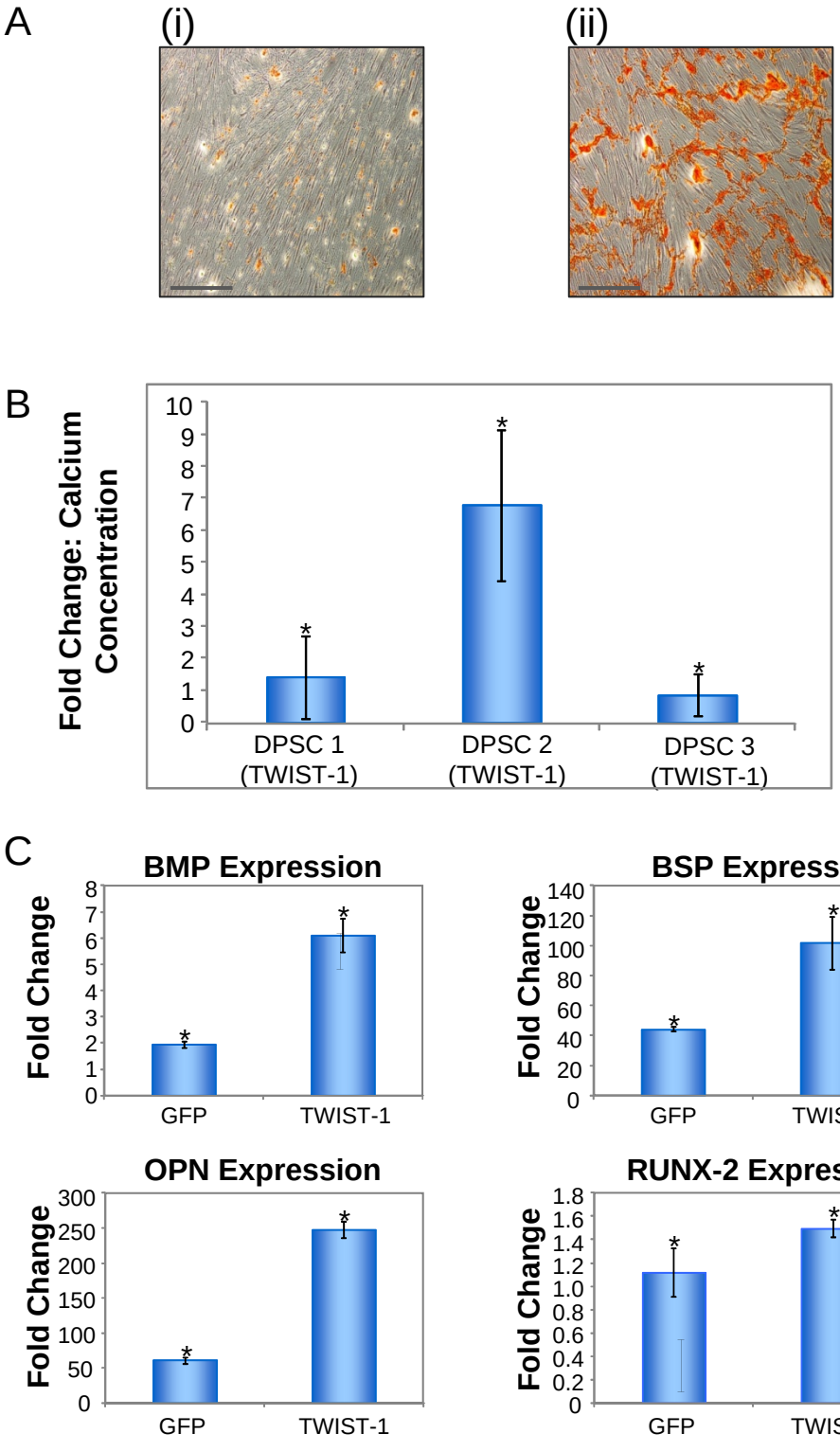
A
(i)
(ii)
B
Fold Change: Calcium Concentration
10
9
8
7
6
5
4
3
2
1
0
DPSC 1 (TWIST-1)
DPSC 2 (TWIST-1)
DPSC 3 (TWIST-1)
C
BMP Expression
Fold Change
8
7
6
5
4
3
2
1
0
GFP
TWIST-1
BSP Expression
Fold Change
140
120
100
80
60
40
20
0
GFP
TWIST-1
OPN Expression
Fold Change
300
250
200
150
100
50
0
GFP
TWIST-1
RUNX-2 Expression
Fold Change
1.8
1.6
1.4
1.2
1.0
0.8
0.6
0.4
0.2
0
GFP
TWIST-1

(**Figure 5.6B)**. Further confirmatory analysis demonstrated an increase in the expression levels of markers associated with osteogenesis, including BMP, BSP, OPN and RUNX-2, in TWIST-1 over-expressing DPSC populations in comparison to vector controls, relative to non-induced control cultures. The data represent the mean values ± standard deviations of triplicate experiments normalised to the house keeping β-actin gene. Statistical significance (*) of $p<0.001$ was determined by the unpaired t-test (**Figure 5.6C**).

When cultured under adipogenic conditions, a decrease in formation of Oil Red O positive lipid clusters (**Figure 5.7A**) and reduced triglyceride levels (**Figure 5.7B**) were demonstrated in TWIST-1 over-expressing DPSCs compared to vector controls and relative to non-induced control cultures. The data in **Figure 5.7B** represent the mean values ± standard deviations generated from TWIST-1 over-expressing DPSCs and vector controls from three donors. Statistical significance (*) of $p<0.05$ was determined by the unpaired t-test. Reduced adipogenic differentiation capacity of TWIST-1 over-expressing DPSCs was further confirmed by decreased levels of expression of ADIPSIN, leptin and PPARγ2 in comparison vector controls, relative to non-induced control cultures. The data represent the mean values ± standard deviations of triplicate experiments normalized to the house keeping β-actin gene. Statistical significance of (*) of $p<0.001$ was determined by the unpaired t-test (**Figure 5.7C**).

In contrast to DPSCs, two out of three of TWIST-1 over-expressing PDLSC populations exhibited a decrease in osteogenic differentiation potential as demonstrated by their reduced capacity to form mineralised nodules (**Figure 5.8A**). Confirmatory quantitative analysis demonstrated reduced levels of calcium present in the extracellular matrix of TWIST-1 over-expressing PDLSCs in comparison to vector controls, relative to non-induced control cultures. The data represent the mean values ± standard deviations generated from TWIST-1 over-expressing PDLSCs and vector controls from three donors. Statistical significance of (*) of $p<0.05$ was determined by the unpaired t-test (**Figure 5.8B**). These results were confirmed using Real-Time PCR, which showed decreased levels of expression of the osteogenic markers BMP, BSP, OPN and RUNX-2 in TWIST-1 over-expressing PDLSCs in comparison to vector controls, relative to non-induced control cultures. The data represent the mean values ± standard deviations of triplicate experiments normalized to the house keeping β-actin gene. Statistical significance of (*) of $p<0.001$ was determined by the unpaired t-test (**Figure 5.8C**).

Figure 5.7 Enforced TWIST-1 Expression Inhibits Adipogenic Differentiation of DPSC

All of the TWIST-1 over-expressing DPSC lines showed a reduced potential to form lipid in comparison to the vector controls. The presence of lipid globules was identified by Oil Red O staining (**A**) (scale bar = 50μm) of (**i**) vector controls and (**ii**) TWIST-1 over-expressing DPSC, cultured under inductive adipogenic conditions. (**B**) Triglyceride levels were measured and normalised to DNA content per well. The data represent values of fold change ± standard deviation of TWIST-1 over-expressing DPSC in comparison to vector controls. (**C**) Real-Time PCR analysis demonstrated reduced levels of expression of markers of adipogenesis, ADIPSIN, LEPTIN and PPARγ2, in TWIST-1 over-expressing DPSC lines in comparison to vector controls, relative to non-induced control cultures. The data represent the mean values ± standard deviations of triplicate experiments normalized to the house keeping β-actin gene. Statistical significance of (*) of $p<0.001$ was determined by the unpaired t-test.

Figure 5.7

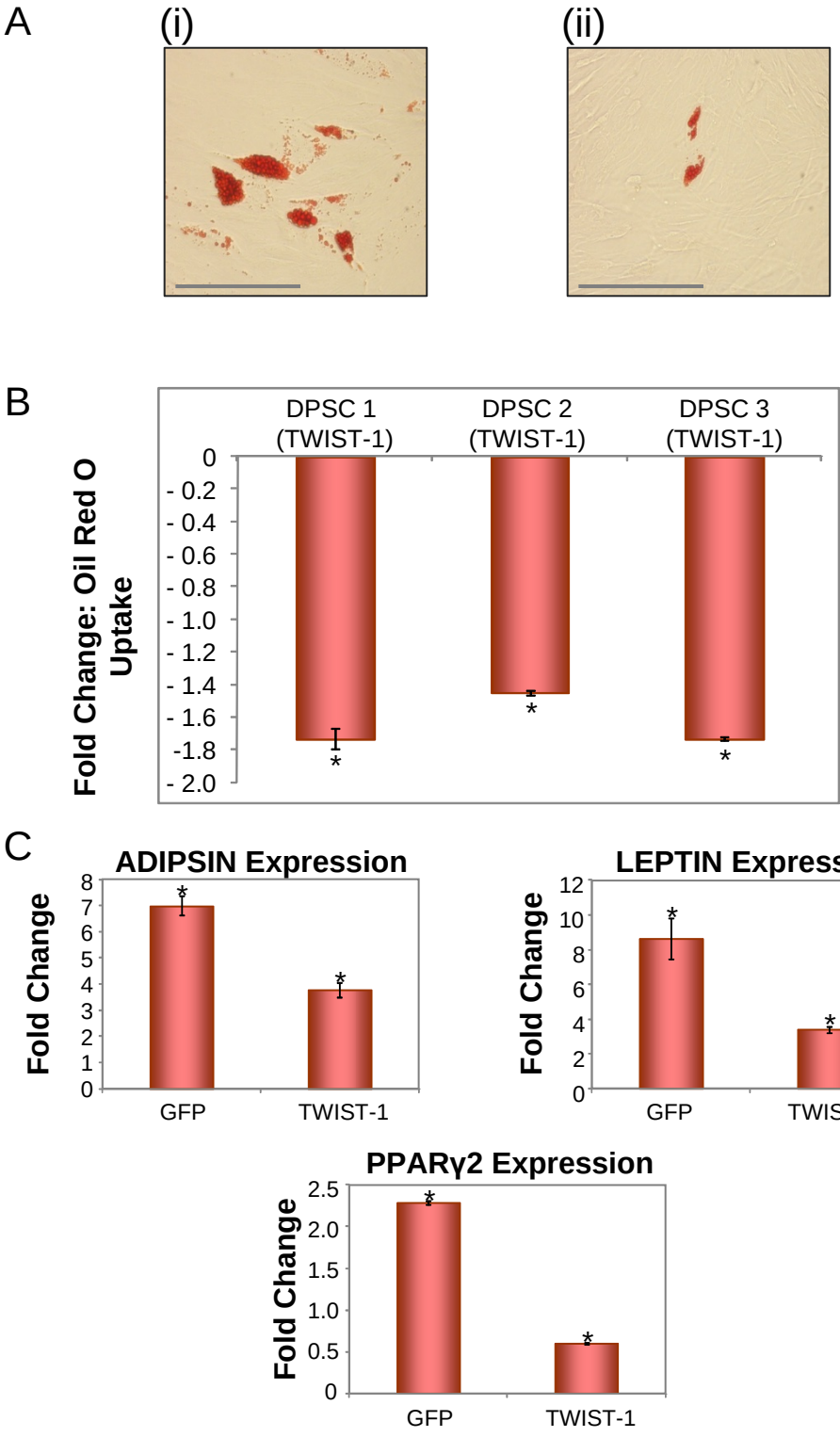
A
(i)
(ii)
B
DPSC 1 (TWIST-1)
DPSC 2 (TWIST-1)
DPSC 3 (TWIST-1)
Fold Change: Oil Red O Uptake
0
- 0.2
- 0.4
- 0.6
- 0.8
- 1.0
- 1.2
- 1.4
- 1.6
-1.8
- 2.0
*
C
ADIPSIN Expression
Fold Change
GFP
TWIST-1
LEPTIN Expression
PPARγ2 Expression

Figure 5.8 Enforced TWIST-1 Expression Inhibits Osteogenic Differentiation of PDLSC

The majority of TWIST-1 over-expressing PDLSC lines showed a reduced potential to form mineral in comparison to the vector controls. The presence of mineral nodules was identified by Alizarin Red staining (**A**) (scale bar = 200μm) of (**i**) vector controls and (**ii**) TWIST-1 over-expressing PDLSC, cultured under inductive osteogenic conditions. (**B**) Calcium concentration within the extracellular matrix was measured and normalised to DNA content per well. The data represent values of fold change ± standard deviation of TWIST-1 over-expressing PDLSC in comparison to the vector controls. (**C**) Real-Time PCR analysis demonstrated decreased levels of expression of markers of osteogenesis, BMP, BSP, OPN and RUNX-2 in TWIST-1 over-expressing PDLSC lines in comparison to the vector controls, relative to non-induced control cultures. The data represent the mean values ± standard deviations of triplicate experiments normalized to the house keeping β-actin gene. Statistical significance of (*) of $p<0.001$ was determined by the unpaired t-test.

Figure 5.8

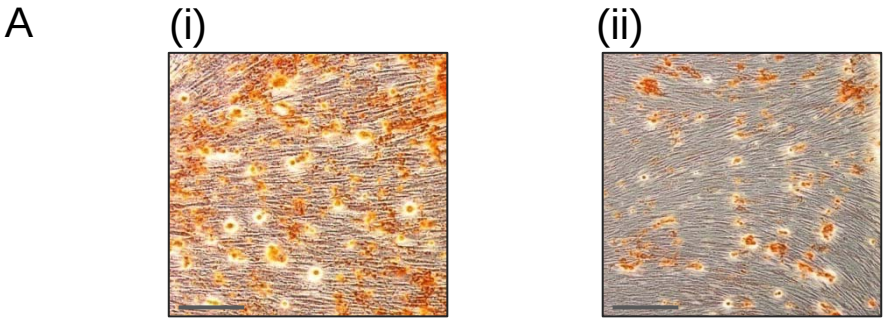
A
(i)
(ii)

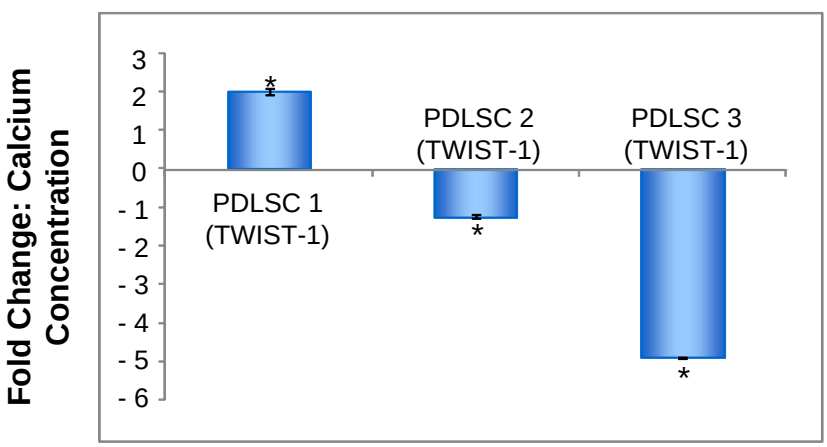
B
Fold Change: Calcium Concentration
3
2
1
0
- 1
- 2
- 3
- 4
- 5
- 6
PDLSC 1 (TWIST-1)
PDLSC 2 (TWIST-1)
PDLSC 3 (TWIST-1)
*
*
*

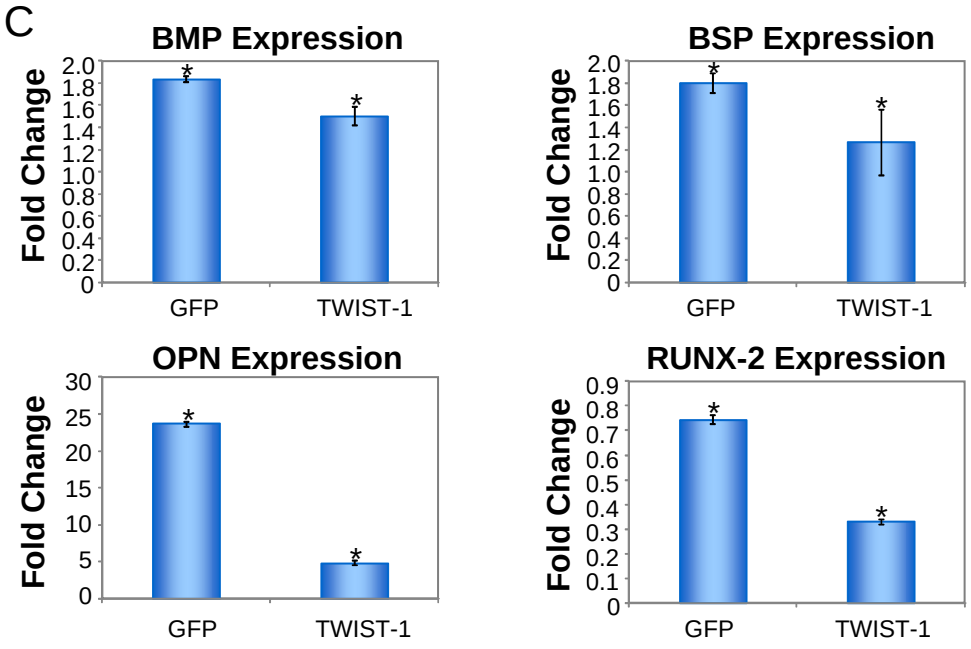
C
BMP Expression
Fold Change
2.0
1.8
1.6
1.4
1.2
1.0
0.8
0.6
0.4
0.2
0
GFP
TWIST-1
BSP Expression
OPN Expression
30
25
20
15
10
5
RUNX-2 Expression
0.9
0.8
0.7
0.6
0.5
0.4
0.3
0.2
0.1

Also in contrast to DPSCs, assessment of the effect of enforced expression of TWIST-1 on the adipogenic differentiation potential of PDLSCs showed an increased potential in the production of Oil Red O positive lipid laden adipocytes in the TWIST-1 over-expressing cultures (**Figure 5.9A**). Quantitative assessment of triglyceride synthesis confirmed the above finding. The data represent the mean values ± standard deviations generated from TWIST-1 over-expressing PDLSCs and vector controls from three donors. Statistical significance of (*) of $p<0.05$ was determined by the unpaired t-test (**Figure 5.9B**). Furthermore, Real-Time PCR analysis demonstrated an increase in the levels of expression of adipogenic markers ADIPSIN, LEPTIN and PPARγ2 in TWIST-1 over-expressing PDLSCs in comparison to vector controls, relative to non-induced control cultures. The data represent the mean values ± standard deviations of triplicate experiments normalized to the house keeping β-actin gene. Statistical significance of (*) of $p<0.001$ was determined by the unpaired t-test (**Figure 5.9C)**.

5.3. DISCUSSION

Findings obtained from an earlier microarray study (**Chapter 4**), identified TWIST-1 as being upregulated across BMSC, DPSC and PDLSC clonal populations of high growth and multi-differentiation potential. This is in agreement with previous work generated by our group that demonstrated high TWIST-1 expression in purified populations of STRO-1^{bright} BMSC, which was downregulated during *ex vivo* expansion [230]. Functional studies also showed that enforced expression of TWIST-1 enhanced the growth potential of BMSC but inhibited osteogenic differentiation, while promoting adipogenesis [230]. We therefore studied the regulatory role of TWIST-1 in DPSC and PDLSC populations.

Figure 5.9 Enforced TWIST-1 Expression Promotes Adipogenic Differentiation of PDLSC

All of the TWIST-1 over-expressing PDLSC lines showed an elevated potential to form lipid in comparison to their vector controls. The presence of lipid globules was identified by Oil Red O staining (**A**) (scale bar = 50μm) of (**i**) vector controls and (**ii**) TWIST-1 over-expressing PDLSC, cultured under inductive adipogenic conditions. (**B**) Triglyceride levels were measured and normalised to DNA content per well. The data represent values of fold change ± standard deviation of TWIST-1 over-expressing PDLSC in comparison to the vector controls. (**C**) Real-Time PCR analysis demonstrated increased levels of expression of markers of adipogenesis, ADIPSIN, LEPTIN and PPARγ2, in TWIST-1 over-expressing PDLSC lines in comparison to the vector controls, relative to non-induced control cultures. The data represent the mean values ± standard deviations of triplicate experiments normalized to the house keeping β-actin gene. Statistical significance of (*) of $p<0.001$ was determined by the unpaired t-test.

Figure 5.9

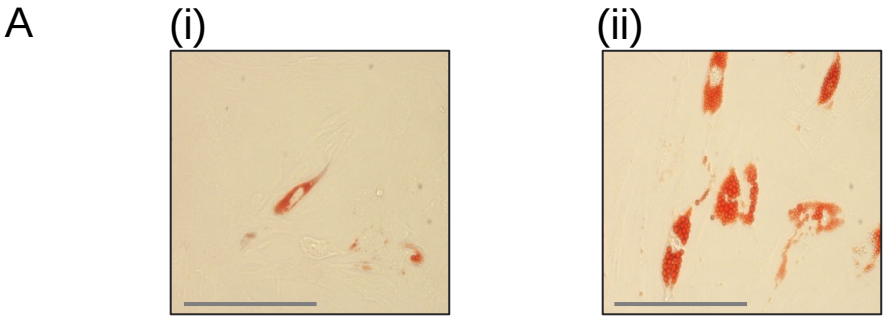
A
(i)
(ii)

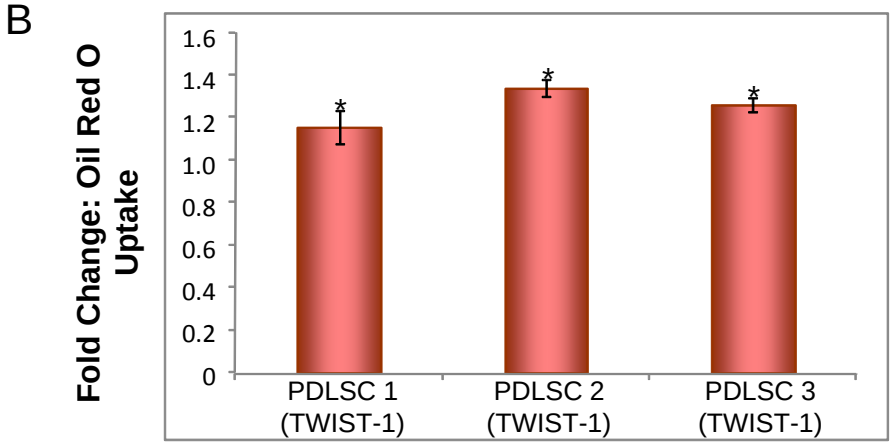
B
Fold Change: Oil Red O Uptake
1.6
1.4
1.2
1.0
0.8
0.6
0.4
0.2
0
PDLSC 1 (TWIST-1)
PDLSC 2 (TWIST-1)
PDLSC 3 (TWIST-1)

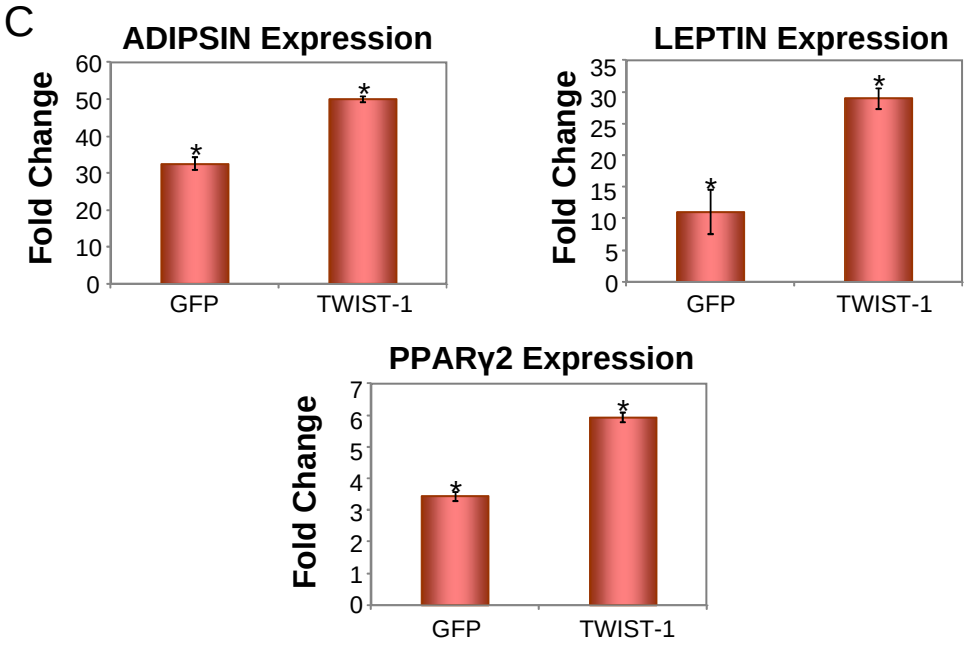
C
ADIPSIN Expression
Fold Change
60
50
40
30
20
10
0
GFP
TWIST-1
LEPTIN Expression
Fold Change
35
30
25
20
15
10
5
0
GFP
TWIST-1
PPARγ2 Expression
Fold Change
7
6
5
4
3
2
1
0
GFP
TWIST-1

5.3.1. Enforced Expression of TWIST-1 Promotes the Proliferation Rate and Increases the Life Span of BMSC, PDLSC and DPSC Populations.

In this study we assessed cellular proliferation and differentiation of TWIST-1 over-expressing dental pulp and periodontal ligament derived MSC bulk populations and compared our findings to those previously reported for BMSC [230]. Similarly to observations reported for BMSC populations, we found that the enforced TWIST-1 expression had an enhanced effect on the rate of cellular proliferation and appeared to increase the life span of MSC-like cells derived from dental pulp and periodontal ligament populations. However, an increased sample size is needed to determine whether the trend towards a prolonged life span in the high TWIST-1 expressing MSCs is statistically significant. Nevertheless, these findings suggest that TWIST-1 mediated cellular proliferation is governed by the same regulatory processes across the three different MSC-like populations. Although the precise mechanisms of these actions still remain to be elucidated, it has previously been suggested that TWIST-1 may regulate proliferation through several mechanisms of regulation of the p53 pathway [369, 370], which transactivates target genes to maintain efficient induction of growth arrest and apoptosis [371, 372]. Moreover, our recent studies demonstrated that enforced TWIST-1 expression was associated with increased ID-1 and ID-2 mRNA levels in BMSC populations [230]. Members of the ID family play a role in positive regulation of G_1 progression and due to their involvement in cell cycle control they promote cell growth [373-376]. Accordingly, the study of Isenmann and colleagues suggested that TWIST-1 regulation of ID-1 and ID-2 led to the observed enhanced cellular growth and increased life span of BMSC [230]. Whilst it is reasonable to propose that the same regulatory mechanism is involved in DPSC and PDLSC populations, the assessment of ID-1 and ID-2 expression levels in TWIST-1 over-expressing DPSCs and PDLSCs would elucidate the relationship between TWIST-1 and ID molecules in these MSC populations.

5.3.2. A Differential Role of TWIST-1 in MSC Differentiation between BMSC, DPSC and PDLSC Populations.

TWIST-1 over-expression studies in BMSC populations demonstrated inhibition of osteogenic differentiation but exhibited an enhanced capacity to undergo adipogenesis, in TWIST-1 over-expressing cells [230]. In the present study, similar findings were seen in

PDLSC populations, however, enforced expression of TWIST-1 in dental pulp derived MSCs resulted in an increase in osteogenesis coupled with a reduction in adipogenic differentiation of these cells. Although MSCs derived from dental pulp have demonstrated the capacity to form calcified tissues *in vivo*, these tissues differ in structure and composition to the bone tissue formed by BMSCs and cementum formed by PDLSCs [41, 97]. As discussed earlier (**Chapter 1, Section 1.2.1.2**) DPSCs demonstrate the ability to form dentin/pulp-like structures *in vivo*, composed of highly ordered collagenous matrix, lined with an odontoblast-like layer, perpendicular to the tubular mineral surface, which surrounds vascularised pulp-like interstitial tissue [24, 377]. On the other hand, PDLSCs exhibit the capacity to form cementum/PDL-like tissues [41] as discussed in **Chapter 1, Section 1.2.1.3**. Cementum is a hard, mineralised tissue [99] laid down in a lamella fashion similar to bone formed by BMSC, where osteoblasts and cementoblasts are positioned in a parallel direction to bone and cementum surfaces, respectively. Therefore, differences in matrix composition and mineral structure imply that the underlying molecular mechanisms that regulate these processes are more similar between BMSC and PDLSC populations, as indicated by the effect of TWIST-1 over-expression which inhibited mineralization for both cell populations, in contrast to DPSCs.

The developmental origin of the different MSC populations [378, 379] may effect their responses to transcriptional regulation by TWIST-1. However, BMSC are derived from the paraxial and lateral plate mesoderm, which give rise to the axial and appendicular skeletons respectively [379], while DPSCs and PDLSCs are derived from migrating neural-crest cells [83, 380]. Therefore, it is not apparent why osteo/cementoblast precursor populations of mesodermal and neural crest origin are regulated by similar signalling pathways, in contrast to DPSCs and PDLSCs. Further comparative microarray assessment of genes unique to either BMSC/PDLSC, BMSC/DPSC and DPSC/PDLSC during normal growth and following differentiation may help identify specific signalling and regulatory pathways involved in the formation of calcified structures by precursor cells derived from different developmental origins.

5.3.3. A Potential Role of TWIST-1 in Interaction of Molecular Regulation Involved in MSC Differentiation into Osteogenic and Adipogenic Lineages

A substantial amount of research has focused on characterising the molecular pathways that regulate the differentiation of MSC. Even though it is evident that TWIST-1 controls osteo/chondrogenic differentiation, the molecular mechanisms and the target genes involved in these processes are still largely unknown. Hayashi *et al* characterised a novel mechanism by which TWIST-1 and ID-1 regulate differentiation of mesenchymal cell lineages by competitive binding to E-protein, through BMP signalling, a pathway vital to osteogenic, chondrogenic and adipogenic differentiation [381-383]. Members of the ID family, are negative acting bHLH factors which lack the DNA binding basic region, and inhibit cellular differentiation by sequestering positive bHLH molecules such as TWIST-1 away from binding to an active promoter region [194, 384]. Hayashi *et al* demonstrated that TWIST-1 inhibits BMP-induced osteogenesis and as such maintains MSCs in their undifferentiated state [381]. They proposed that TWIST-1 exerts its inhibitory effect possibly indirectly, through the inhibition of RUNX-2 or directly, by forming heterodimers with E protein and inhibition of SMAD mediated transcriptional activity, critical to BMP signalling [381]. Additionally, TWIST-1 plays an inhibitory role in chondrogenesis manifested by the induction of TWIST-1 through Wnt signalling, which results in repression of chondrogenic gene expression [385]. It was further suggested that TWIST-1 is a potent inhibitor of chondrogenic differentiation potentially and partially through its suppression on RUNX-2 [386].

Previous studies have suggested that autocrine TGFβ signalling controls differentiation of mesenchymal stem cells and that the expression of TGFβ receptors is augmented during differentiation processes to enable maturation into cells of specific lineages [387, 388]. Zhou *et al* demonstrated that chondrogenic differentiation of human MSCs was promoted by the activation of the TGFβ/SMAD signalling pathway, which further inhibited adipogenesis in these cells [389]. Moreover they proposed the involvement of Wnt signalling in these processes, which either independently or cooperatively with TGFβ signalling resulted in the observed stimulatory and inhibitory effects [389]. In their later studies, they showed that the differentiation of human MSCs into cells of adipogenic lineage was inhibited by TGFβ signalling, as induction with TGFβ-1 resulted in down-regulation of PPARγ and lipoprotein lipase (LPL) gene expression in the assessed MSC

populations [390]. These studies were confirmatory to the previous findings of Choy and colleagues which found TGFβ signalling had an inhibitory role in adipogenesis, where the availability for TGFβ receptors was strongly down-regulated during adipogenic differentiation [391].

Reinhold *et al* identified TWIST-1 as a transcriptional target of canonical Wnt signalling that repressed chondrocyte gene expression. Their findings suggested that TWIST-1 inhibited chondrogenesis by Wnt signalling but could also induce changes to chondrocyte gene expression through BMP dependent pathways [385]. Moreover, studies conducted by Dong *et al* suggested a stage specific mechanism associated with TWIST-1 and RUNX-2 regulation of molecular events occurring between immature and hypertrophic chondrocytes [386]. They found that the differentiation of progenitors into hypertrophic chondrocytes only occurred when TWIST-1 levels, which are high in immature cells, were decreased and RUNX-2 expression was increased to facilitate terminal maturation. They proposed that TWIST-1 exerts its effects through TGFβ and canonical Wnt signalling pathways [386].

The role of canonical Wnt-β-catenin signalling pathway is essential to skeletogenesis and skeletal remodelling, due to its regulation of numerous processes including stem cell renewal, stimulation of osteoblast proliferation and induction of osteoblastogenesis [392, 393]. Conversely, activation of β-catenin affects transcriptional activation of the adipogenic transcription factors, C/EBPα and PPARγ [394] and blocks the induction of these factors through canonical Wnt signaling, resulting in inhibition of adipogenesis [395-399]. A study by Pan *et al* demonstrated that TWIST-1 plays a role in the negative feedback regulation in brown fat metabolism [400]. TWIST-1 was identified as a specific inhibitor of PGC-1α, a principal regulator of brown fat thermogenesis. *In vitro* experiments illustrated that PGC-1α activity was inhibited through direct interaction with TWIST-1, which in turn modulated oxidative metabolism [400]. *In vivo* studies showed that transgenic mice over-expressing TWIST-1 were susceptible to high-fat diet induced obesity whereas heterozygous TWIST-1 knock-out mice exhibited resistance to obesity. Moreover, it was suggested that the actions of TWIST-1 and PGC-1α were coordinated by PPARδ, as it was demonstrated that PPARδ bound to the promoter of TWIST-1 and regulated its expression [400].

Collectively, these studies illustrate an inverse relationship between the regulatory mechanisms of osteo/chondrogenic and adipogenic lineage commitment and differentiation processes. Based on these findings, it is reasonable to suggest that TWIST-1 potentially exerts its effect on MSC differentiation, via its reciprocal regulation through the BMP, TGFβ and Wnt signaling pathways. Our findings generated for PDLSCs were consistent with previously assessed BMSC populations [230], and were in accord with an earlier study, where TWIST-1 was found to suppress osteogenesis in periodontal ligament derived cells [368]. In contrast, TWIST-1 appeared to play an opposing role in the osteogenic and adipogenic differentiation of DPSCs, suggesting that TWIST-1 exhibits alternate regulation of different MSC-like populations.

Whilst beyond the scope of this study, these findings lay the foundation for future work, essential to deciphering the different mechanisms that control and regulate processes vital to MSC growth and development. To obtain greater insight into the regulatory mechanisms of TWIST-1 mediated growth and development, knock-down studies could be performed in high growth and multi-differentiation potential clonal MSC populations using shRNA technology, isolated in our earlier experiments (**Chapter 3**). Parallel over-expression and knock down studies could also be performed for the other transcription factors E2F-2, LDB-2 and PTTG-1 commonly expressed by high proliferative, multi-potential BMSCs, DPSCs and PDLSCs. Further interrogation of the microarray data may lead to the identification of putative gene targets for TWIST-1 and E2F-2, LDB-2 and PPTG-1 to help determine the downstream events that lead to functional changes observed in the different MSC-like populations.

Chapter 6:

General Discussion

6. Discussion

In this study clonal populations of long-lived, multi-potential MSCs were isolated from the bone marrow, dental pulp and periodontal ligament tissues. Their unique gene expression profiles were assessed to identify a set of genes commonly upregulated amongst multi-potential BMSC, DPSC and PDLSC populations.

6.1. The Rationale of the Project

Mesenchymal stem cells (MSCs) reside within a number of organs in the body where they play a role in tissue regeneration and homeostasis. MSCs were initially identified in the bone marrow [34, 35], and subsequently, MSC-like cells have been obtained from dental pulp and periodontal ligament tissues [24, 41]. These cells hold great potential for tissue regeneration in clinical applications as they are easily accessible, immunocompatible and exhibit high growth and differentiation capacity. However, a number of technical issues, including identification and isolation of the optimal precursor cell populations, need to be addressed to achieve the desired therapeutic outcome.

Currently, a major limitation in the clinical use of MSCs is the difficulty in obtaining defined initial cell preparations, coupled with the heterogeneity of the starting cell population. Based on this, we set out to investigate clonal MSC populations isolated from bone marrow, dental pulp and periodontal ligament through functional and genomic characterisation of these populations.

Gene expression profiling has been used to identify many candidate molecular biomarkers or classifier genes which may be used for predicting unique phenotypic features of a given cell population [185, 186]. Therefore, this technology was applied to obtain reliable data sets that define vital processes involved in MSC growth, survival and development. In addition, assessment of the differential gene expression patterns was carried out to identify significant molecular differences and unique biological markers specific to our target MSC populations.

Overall, the aim of this project was to gain insight into the fundamental cellular processes involved in stem cell maintenance, growth and development. This was achieved by the assessment of gene expression profiles of MSCs of differing developmental potential,

derived from different origins, and the identification of key global factors involved in MSC proliferation and differentiation.

6.2. Result Summary and Discussion

Initial findings of the present study highlighted the importance of characterisation of MSCs at the clonal level as it allowed determination of specific stages of development and addressed the issue of heterogeneity within MSC populations. Consequently, clonal populations of low growth capacity and high growth/multi-differentiation potential were identified within bulk cultures of BMSCs, DPSCs and PDLSCs. Although only a small fraction of BMSCs exhibited high proliferative potential, greater proportions of DPSCs and PDLSCs exhibited an extensive proliferation capacity and an ability to exceed 20 population doublings. Furthermore, essentially all highly proliferative BMSC clonal lines exhibited a capacity to differentiate into cells of osteogenic, chondrogenic and adipogenic lineages. Conversly, multi-lineage differentiation potential was observed for only 50% of the highly proliferative DPSC and PDLSC clones. It is proposed that the differences observed in growth and developmental potential across the three MSC-like populations may be associated with the different, mesodermal and ectomesenchymal, developmental origins of BMSC and dental MSCs, respectively. These findings confirmed the heterogeneity of MSC populations in reference to their differentiation and proliferation capacities and further illustrated the hierarchical nature of stromal MSCs. These initial experiments provided the basis for further characterisation of identified clonal populations and enabled assessment for identification of unique markers that could be used for the isolation and expansion of highly proliferative, multi-potential MSC subpopulations.

Whole genome arrays were used to assess gene expression profiles of clones exhibiting functional differences across MSC populations derived from three stromal tissues. Initial comparative analyses of clonal PDLSC populations were carried out using two commercially available platforms, Affymetrix® U133 and Illumina® WG-6. A similar number of differentially expressed genes was identified between the different clonal populations, assessed using the two platforms. Additionally, approximately 40% of the identified genes were common to analyses performed on both of the platforms. Considering the comparable outputs of the two microarray systems, and based on the specific configuration of the BeadChip® designed by Illumina, this platform was used for subsequent analyses. The results obtained from gene expression profiling of selected MSC

populations suggested that a coordinated action of numerous genes is involved in control of multiple signalling pathways which regulate proliferation and differentiation of MSCs. These findings are in accord with previous studies which suggested that a cohort of genes may be associated with stem cell functions and involved in pathways that control stem cell maintenance and proliferation potential. Specifically, the findings implicated E2F-2, LDB-2, PTTG-1, and TWIST-1 as potential key transcriptional factors or co-factors that may mediate maintenance, growth and development of mesenchymal stem-like cells derived from different anatomical sites.

In a proof-of-principal study, the regulatory role of TWIST-1 in bulk DPSC and PDLSC populations was studied and was based on the previously reported involvement of TWIST-1 in BMSC growth and commitment [230]. Interestingly, TWIST-1 expression has been found to be associated with immature mesenchymal populations and down regulated in committed progeny [230, 334, 339, 346]. Corresponding with observations reported for BMSC populations, we found that enforced TWIST-1 expression had an enhanced effect on the rate of cellular proliferation and appeared to increase the life span of MSC-like cells derived from dental pulp and periodontal ligament populations. However, more replicate samples are required for establishing statistical significance in the increase trend for life span in the TWIST-1 expressing DPSC and PDLSC. Furthermore, comparable with the demonstrated effect in BMSC populations, the findings of the present study indicated that enforced TWIST-1 expression inhibited osteogenic differentiation, whilst promoting adipogenesis in bulk PDLSC populations. Conversely, enforced TWIST-1 expression increased the capacity of DPSC bulk populations to mineralise *in vitro* while inhibiting their ability to undergo adipogenesis. Whilst the reasons for the disparities in TWIST-1 mediated differentiation between BMSC/PDLSC and DPSC is unclear, differences in the functional outcome may be due to the tissue origin of each cell type and the mechanisms that they employ to undergo mineralization, as calcified bone/cementum matrices have a different pattern of crystal deposition to that of dentine.

In light of this, it is suggested that TWIST-1 is an important stimulator of MSC proliferation and that its molecular regulation mechanism may vary across MSC populations derived from different stromal tissues, accounting for the differential effects exerted on the developmental potential of these cells.

6.3. Future Directions

6.3.1. Further Functional Characterisation of Clonal MSC Populations

Initial studies identified clonal populations of BMSC, DPSC and PDLSC of low growth and high growth/tri-differentiation potential by assessing their proliferation potential and the capacity of these cells to differentiate into cells of osteogenic, chondrogenic and adipogenic lineages *in vitro.* Further assessment that would provide a more distinct indication of the differentiation potential of cells of high growth capacity would involve testing the ability of these clonal populations to differentiate into other cell lineages, including haematopietic supportive stroma, the myoblasts and neural cells. Additionally, *in vivo* assessment of the proliferation and differentiation capacity of highly proliferative MSCs would further delineate these populations and identify more distinct cell subsets with the capacity to generate an active bone marrow organ following subcutaneous transplantation into immunocompromised mice using an appropriate osteoconductive carrier [12].

6.3.2. Proteomic Profiling of MSC Populations

To confirm the findings of the microarray data, and to further identify markers unique to MSC populations of high potential, comparative proteomic analysis could be performed for clonal MSC populations of low growth and high growth/multi-differentiation potential [401]. Generation of proteomic expression profiles would give further, valuable insight into the molecular regulation involved in these MSCs as the data obtained using this technology would identify post-translation protein modifications which are not detected by microarray analyses.

6.3.3. Further Assessment of the Microarray Data

Due to the extent of the data volume obtained through the whole genome microarray analysis approach, data interrogation was limited and, more importantly, further experimental analysis of the identified genes sets was restricted. Additional examination of the microarray data may identify potential gene targets for TWIST-1, E2F-2, LDB-2 and PTTG-1 to further elucidate the regulatory mechanisms that led to the observed functional changes in the assessed MSC populations.

6.3.4. TWIST-1 Knock-Down Studies in MSCs of High Growth Potential

Knock-down studies of TWIST-1 in MSC population of high growth capacity would further characterise its molecular interactions and highlight the importance of this factor in MSC proliferation and differentiation processes. Together, with the results obtained for the TWIST-1 over-expression studies, these findings would, to a greater extent, decipher the involvement of TWIST-1 in MSC development.

6.3.5. Over-Expression and Knock-Down studies of E2F-2, LDB-2 and PTTG-1 in MSCs of High Growth Potential

Enforced increase and/or reduction of the expression levels of the other transcriptional regulators commonly upregulated in MSCs of high capacity, followed by functional analysis, would elucidate the role of E2F-2, LDB-2 and PTTG-1 in cellular proliferation and differentiation processes of MSCs.

6.4. Concluding Remarks

In this study functional and molecular characterisation was carried out on clonal MSC populations derived from different stromal tissues. The capacity of these cells to readily differentiate into multiple lineages offered an ideal model to identify key molecular switches involved in MSC lineage commitment using gene expression profiling.

Amongst large microarray data sets, a cohort of genes associated with stem cell-like characteristics was identified. Ongoing investigations seek to examine the significance of this gene set as a signature of early mesenchymal stem cell populations derived from different tissues. This work lays the foundation for identifying novel mesenchymal stem cell markers and/or key regulators of self-renewal, growth and commitment. Furthermore, comprehensive knowledge of the factors and mechanisms involved in these cellular processes will assist in the clinical application of MSCs and development of stem cell-based cell therapies.